International Journal of Surface Engineering and Interdisciplinary Materials Science
Volume 9 • Issue 2 • July-December 2021

Oriented Type I Collagen - A Review on Artificial Alignment Strategies

Karina Ambrock, University of Western Ontario, Canada
Bernd Grohe, Lawson Health Research Institute, Canada
Silvia Mittler, University of Western Ontario, Canada

ABSTRACT

Collagen is the most abundant protein in the human body and serves many functions, from mechanical stability and elasticity in tendons and bone, to optical properties, such as transparency and a fine tuned refractive index in the cornea of the eye. Collagen has interested humankind for centuries: Leonardo Da Vinci studied and drew the tendons in the human body precisely in the 15th and 16th century. A look at the literature reveals easily > 200,000 papers. This article reviews oriented type I collagen artificial alignment strategies.

KEYWORDS

Artificial Alignment, Chemical and Physical Methods, Collagen, Natural Alignment, Natural Structures, Orientation Distribution in 1D, 2D, and 3D, Type I

1. INTRODUCTION

1.1. Background

1.1.1 Collagen Basics

The most abundant protein in mammals, collagen, exists within the extracellular matrix (ECM) providing structure and support to connective tissue. Collagen plays an important role in the formation of tissue and organs (Abraham et al., 2007). It can be found in tendons, ligaments, skin, bone, teeth, cartilage, blood vessels, nerves and organ capsules. Collagen is surface active, biodegradable and excellently biocompatible, even when retrieved from animal resources, making it a candidate material for various biomedical applications (Lee, 2001). Collagen accounts for approximately 20 - 30% of the total protein in a human body (Harkness, 1961; Shoulders, 2009). Currently, over 28 distinct collagen types have been discovered, with various properties, and from various body regions (Shoulders, 2009; Gelse, 2003; Kühn, 1986; Sherman, 2015). Complexity and structural diversity, splice variants, presence of non-helical domains, assembly and function are factors considered in collagen type classification (Gelse, 2003). The general groups of collagen include: fibrillar collagens, FACIT (Fibril Associated Collagens with Interrupted Triple Helices) and FACIT-like collagens, beaded filament collagens, basement membrane collagens, short chain collagens, transmembrane collagens, and others with unique functions (Gelse, 2003; Sherman, 2015). The most common group in the human body, making up nearly 90% of the total collagen, is the fibrillar collagens, consisting of Types I, II, III, V and XI (Gelse, 2003; Hulmes, 2008; Ottani, 2002). The most common form in mammal tissue is type I (Hulmes, 2008). Collagens, type I in particular, are most commonly used in research due to

DOI: 10.4018/IJSEIMS.2021070106

their ability to form highly oriented, structural hierarchies of fibrils and their prevalence in human tissue (Gelse, 2003).

This article focuses on type I collagen only. In an evaluation and rating free fashion it reviews the diverse methods demonstrated to fabricate artificial type I oriented collagen in 1D, 2D and 3D architectures, mimicking natural structures and the achieved orientation, as well as orientation distribution and/or order. In the following type I collagen will often be referred to as just collagen.

1.1.2. Collagen Hierarchy

Type I collagen molecules consist of two α1 chains and one α2 chain that form a right-handed triple helix around an axis (Figure1a and b) (Gelse, 2003, Sherman, 2015; Ottani, 2002; Kadler, 1996; Chattopadhyay, 2014). These three polypeptide chains consist of nearly one thousand residues whereby glycine occurs as every third residue (Gelse, 2003; Ottani, 2002; Kadler, 1996; Chattopadhyay, 2014). The "collagenous" structure of amino acids is commonly expressed as a repeating triplet of Gly-X-Y, where X and Y can be any amino acid; however, it has been reported that the most frequently occurring amino acids in the triplet are proline and hydroxyproline (Kadler, 1996; Chattopadhyay, 2014; Ramshaw, 1998). At the beginning of the *in-vivo* synthesis (Figure1b), the protein exists as procollagen, with a triple helix and two globular terminals. The terminals are cleaved by specific proteases, which leave a triple helix with some terminal non-helical portions (Figure1 c and d). The assembly is now called tropocollagen (molecule). It has a diameter of ~1.6 nm and a length of ~300 nm, and can be viewed as a nanoscopic rod. It can undergo spontaneous fibrillogenesis (Ottani, 2002; Olsen, 1963) via an entropy-driven self-assembly process of the tropocollagen into fibrils (Ottani, 2002; Kadler, 1996).

The type I collagen assembly to form fibrillar collagen is unique because it possesses a staggered, quasi-hexagonal arrangement (Vuorio, 1990). The tropocollagen, staggered by multiples of 68 nm, is called a D-period (Vuorio, 1990). Within one D-period, there are five molecules in cross-section: each molecule staggered by one D-period (Figure1e) (Sherman, 2015; Ottani, 2002; Olsen, 1963). Within each D-period, there is a gap of ~36 nm, and an overlapping region of 31 nm between adjacent molecules (Figure1e) (Vuorio, 1990). Following the self-assembly into the D-period, the tropocollagen becomes cross-linked *in-vivo* by an enzyme. This enzyme undergoes a reaction with the amine side chains of lysine and hydroxylysine and converts the residues into aldehydes (Smith, 1968; Pinnell, 1968; Kruger, 2013). After a hydration reaction the two collagen molecules are cross-linked via peptide bonds. These collagen micro-fibrils further self-assemble into fibrils, and finally into larger macroscopic units called fibers (Figure1f).

1.1.3. Mechanical Properties

The packing of fibrils in a fiber may vary from one tissue to another and influences the mechanical properties. The internal structure of the collagen fibrils and fibers is highly ordered, thus has highly anisotropic physical properties. One distinct property set is the mechanical characteristics, which are used by nature in connective tissue. Numerous studies on mechanical properties of collagen have been performed: both experimentally and theoretically (Fratzl, 2008). Collagen exhibits strength and elasticity that vary with respect to orientation when a constant force is applied. The Young's modulus for collagen fibrils has been measured along the fibrils and values from 0.2 MPa to 12 GPa were found depending on the source of the fibrils (e.g. rat tail, tendon, fish scales, bone, animal, human, etc), their dehydration state, the degree of cross-linking and their multiple hierarchical levels (molecular, fibril, fiber, tissue) (Sherman, 2015; Wenger, 2007; Hamed, 2010). The Young's modulus in the direction perpendicular to the fibrils was not measured satisfactorily yet, due to experimental uncertainties and the interference between the mechanical measurement tools as well as the internal structure of the fibrils (Sherman, 2015; Annaidh, 2012). Indirect measurements have been performed with tissue, e.g. with human skin, selecting samples oriented perpendicular and parallel to the Langer lines (Annaidh, 2012). Langer lines correspond to the natural orientation of collagen fibers in the

Figure 1. Type I collagen consists of a) two identical α1(I) and one α2(I) peptide chains; b) self-assembly to form procollagen; c) in vivo procollagen peptidase removes the loose termini creating, d) type I tropocollagen. Tropocollagen undergoes a second self-assembly process, e) forming collagen fibrils with a D-period, and f) by yet another self-assembly process, collagen fibrils form a collagen fiber (Kruger, 2013). This work is licensed under Creative Commons Attribution 3.0 Unported).

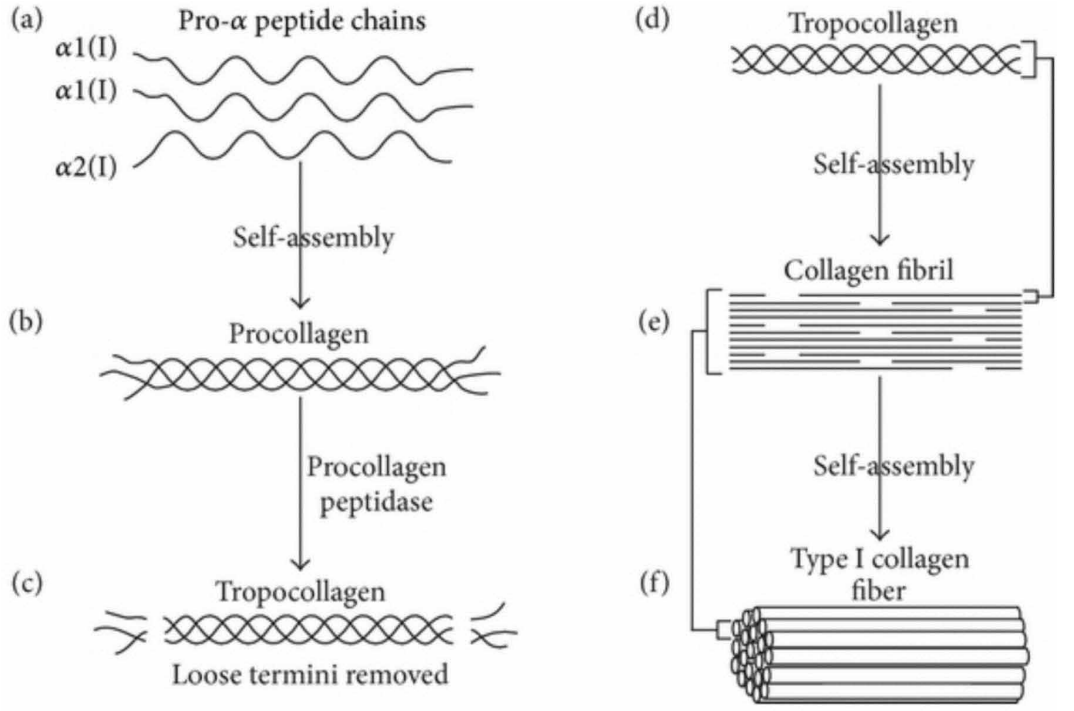

dermis. A difference in the elastic moduli of the two directions of roughly 50% (a relatively large error) was found (Annaidh, 2012).

All collagen-based tissues exhibit non-linear visco-elastic properties, reflected by a "J"-shaped stress - strain curve: collagen exhibits greater compliance at low stresses than at higher stresses. This enhances the energy absorption capacity at low-stress levels. A greater compliance at the onset of loading in combination with some viscous damping are the main properties of collagen reducing the susceptibility to damage (Fratzl, 2008).

2. ALIGNED COLLAGEN IN NATURE: THE DIFFERENT ALIGNMENTS AND CORRESPONDING ORGANS

Collagen as a highly anisotropic material can be assembled in tissue by conserving the high anisotropy via the alignment of all fibrils and fibers in parallel. However, the fibers can also be randomly associated resulting in a more homogeneous tissue; or a preferential fiber orientation can change from layer to layer in a tissue. Woven structures, where fibers mimic a woven fabric, are also assembled.

The form of alignment within a tissue depends on the tissues' function and mechanical (and/or optical) demand. A variety of alignment strategies are found in the human body: parallel, woven, interwoven, plywood-like, radial and circumferential (Fratzl, 2008). Sometimes two or more orientation motives are present at close proximity (Fratzl, 2008).

Figure 2. Collagen assembly hierarchy in tendons, including typical sizes and suitable imaging technologies, the crimp waveform is shown at the fibre level as well as cell presence in fascicles. PGs are proteoglycans which hold water with the help of negative charges and the hydrophilicity of their polysaccharide side-chains (Harvey, 2009): courtesy of Sir Michael Brady).

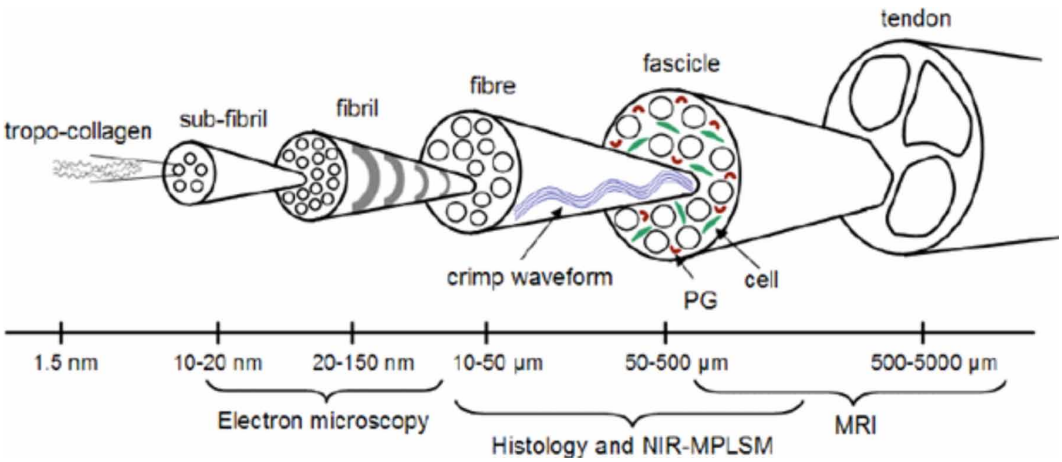

2.1. Parallel: Tendon, Ligament, Bone

Tendons and ligaments are dense, regular connective tissue structures (bands, cords, or straps) (Weintraub, 2003). Ligaments connect bone to bone, while tendons connect muscles to bone. Tendons contain completely parallel bundles of collagen fibers, which provide high unidirectional strength. Ligaments exhibit nearly parallel oriented bundles of collagen fibers with a wavy pattern (crimping), which makes them able to withstand loads in different directions and allows elongation of fibers before tensile stresses are experienced. Tendons show larger collagen fibers than ligaments (Simon, 1994).

However, there is a large tendon-to-tendon variability and tendon site-to-site variation: some tendons also exhibit wavy pattern (Kannus, 2000; Amiel, 1988), but with typically longer crimping periods in comparison to ligaments (Amiel, 1988). Collagen fibrils are sometimes oriented not only longitudinally but also transversely and horizontally, with the longitudinal fibrils also crossing each other, thus forming spirals and plaits. This complex ultrastructure of tendons provides a good buffer capacity against longitudinal, transversal, horizontal, as well as rotational forces during movement and activity. The frequently observed twists and intertextures of the tendon fibers are related to optimal transmission of the forces in certain anatomic points.

Due to their highly oriented fiber arrangement, tendons and ligaments are particularly adapted to resist tensile loads. Ligaments and tendons exhibit visco-elasticity. Similar to purely elastic materials, they can regain their original shape following deformation, after removal of the deforming load. When an elastic material is stretched, work has been done on it, which increases its energy. The material stores this energy and keeps it available, enabling it to recoil back to its original shape (Figure 2).

Bones consist mainly of type I collagen fibrils, dahllite (carbonated apatite) or hydroxyapatite crystals, and water. In bone the mineralized collagen fibrils are almost always present in bundles or arrays aligned along their lengths. The collagen fibrils in bone are generally about 80 –100 nm in diameter. The crystals of bone are plate-shaped, with average lengths and widths of 50 x 25 nm, and are very thin, with thicknesses appearing to be remarkably uniform. Their smallest dimensions vary from just 1.5 nm up to about 4 nm for some mature bone types. Water is located within the fibril, in the gaps, and between tropocollagen. It is also present between fibrils and between fibers. The three major components of bone have completely different properties, therefore bone is a composite. The host is the collagen fiber, formed by fibrils with an internal crystalline structure of orthotropic symmetry (Weiner, 1998). The mineral is located mainly within the gap regions of collagen fibrils. Arrays of parallel fibrils are found in the micron and even millimeter scale size ranges in *parallel-fibered bone* (Weiner, 1998, Feng, 2010).

Figure 3. Part of the hierarchical structure of collagen in cortical bone: a) Lamellas folded around a Haversian canal (containing blood vessels) forming spiraling fiber orientation with a plywood motive in osteons. b) Cortical bone formed by parallel aligned osteons (Feng, 2010).

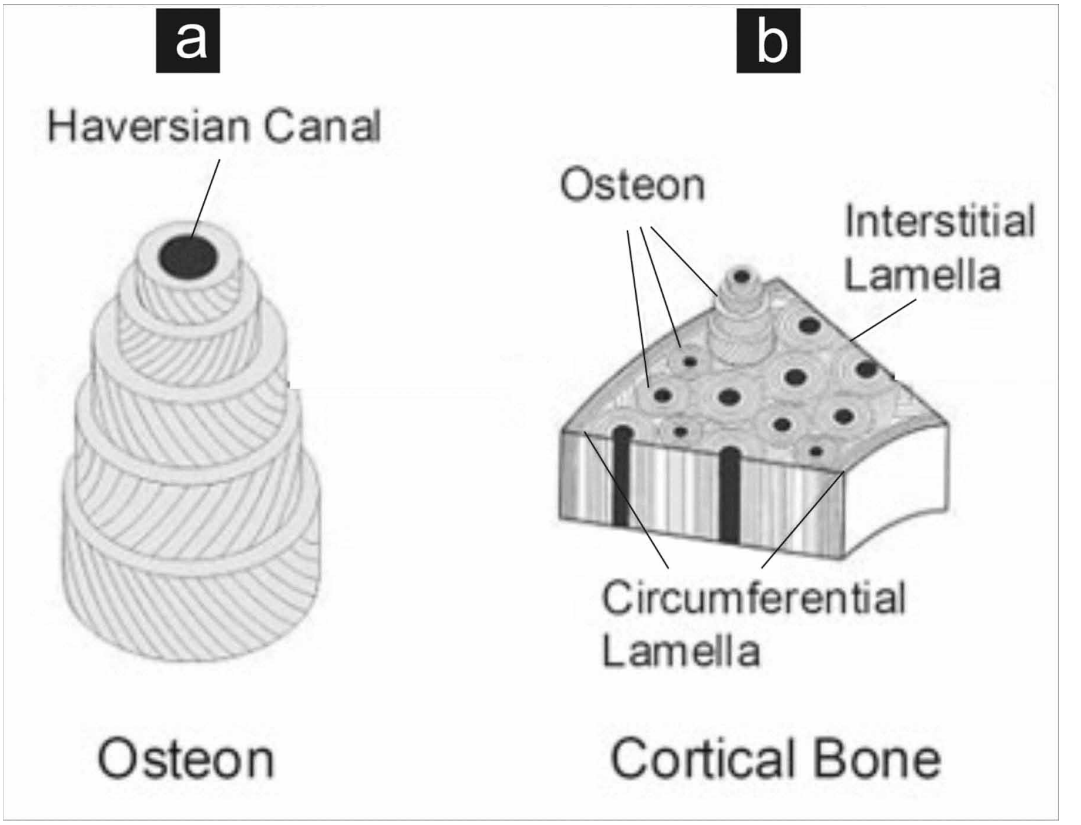

However, *lamellar bone and fibrolamellar bone* also contain parallel arrangements of collagen as depicted in Figure 3. Here the internal structure of collagen within a lamella is parallel, but from lamella to lamella there is a distinct angle between collagen orientation directions (Marlow, 2007; Currey, 2002). In osteons, which are cylindrical aggregates of bone lamellae around blood vessels (Figure 3), the twisted plywood motif results in a spiraling of the fiber orientation around the central blood vessel. Analogous to a spring construction, this structure has biophysical significance in absorbing mechanical energy and protecting the sensitive inner blood vessel from cracks in the interstitial bone (Fratzl, 2008).

2.2. Woven and Interwoven: Healed Bone, Juvenile Bone, Skin, Scelera

In woven collagen structures (Figure 4), the fibrils are arranged into bundles with large variety in diameter. The fibril bundles are loosely packed and poorly oriented. These structures occur *in healing bone* after fracture (Fratzl, 2008), fetus (growing) bones *(*Weiner, 1998) and in parts of the skin (Ramachandran,1976; Brown, 1972), displaying a large multidirectional deformability.

The *sclera* (the white part of the eye) is a tough connective tissue and is connected with the cornea. *Scleral* collagen is, in composition and arrangement, similar to that present in *skin*, with wider fibrils and an interwoven structure (Fratzl, 2008). Interwoven means structures where the collagen fibrils and bundles have connective points via loops (like knitting or a mesh) and/or are arranged like in a thread of span wool.

Figure 4. Scheme of woven collagen structure

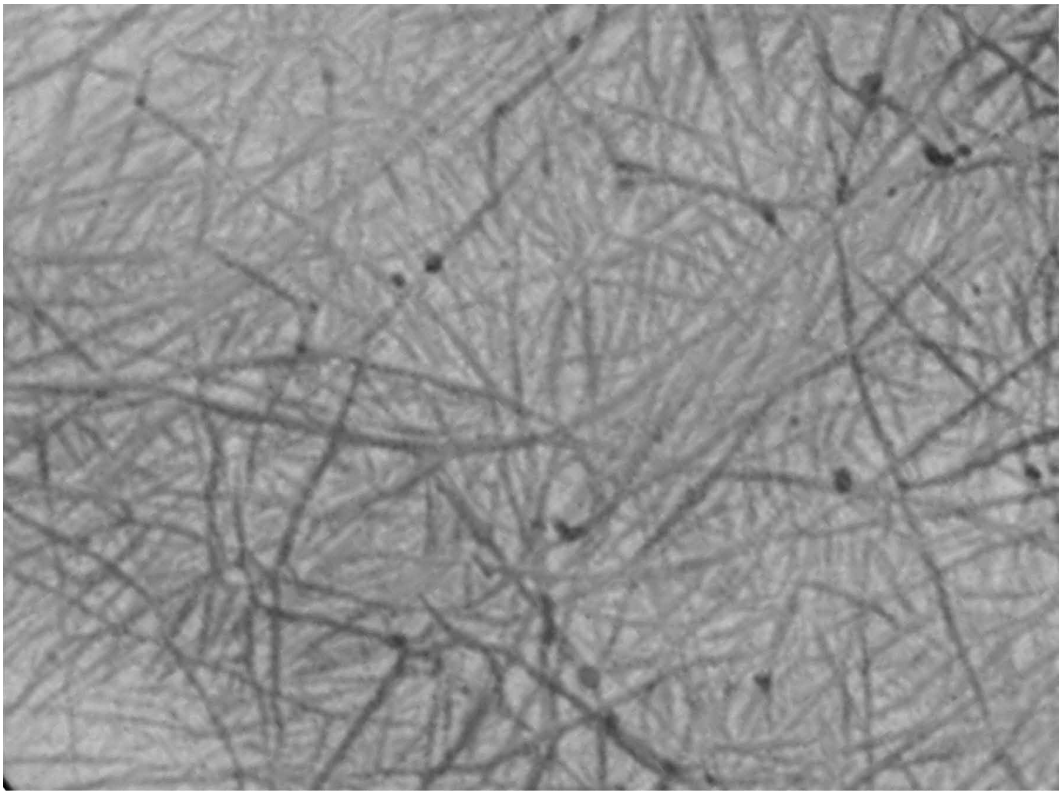

2.3. Plywood-Like: Cornea

Most collagen in the *cornea* is found in the *stroma*. In the *corneal stroma*, collagen is positioned within structures – so-called lamellae (Figure 5) – that occur parallel to the tissue surface and show a collagen orientation parallel to the lamella (with a slight angle to neighboring lamella), producing a plywood-like structure. Lamellae vary in size, but they are typically about 2 μm thick and up to 0.2 mm broad (Komai, 1991; Polack, 1961). These lamellae, except of outermost layers, run in belts across the cornea from limbus (border of the cornea and the sclera) to limbus ((Fratzl, 2008). See also Figure 3: osteon and related text.

2.4. Radial and Circumferential: Dentin

In the case of radial and circumferential orientation one needs to be very careful with the nomenclature, which seems to be different in the collagen sub-communities (bones, arteries, cartilage, etc.). A quasi circumferential fibril array is found in *dentin*: the fibers run around the holes (circumferential), but not in a perfect circle (Weiner, 1999). Dentin is a calcified tissue and forms teeth together with enamel, cementum, and pulp. In the original paper of Weiner et al. (1999) the collagen orientation is named radial.

Arterial walls are composed of three mayor layers (from inside out): intima, *media* and adventitia. The *media* consists of a complex three-dimensional network of bundles of collagen fibrils, which are organized in a varying number of medial lamellar units, each of which about 10 μm thick. The orientation of the collagen fibrils constitutes a continuous fibrous helix (like a screw). The helix has a small pitch leading to an almost circumferentially orientation.

Figure 5. Sketch of the cross-section through five lamellae of a human cornea. Fibrils in adjacent lamellae align in large angles to one another: fibrils are seen in cross-section (dots) and in transverse section (elongated). For an electron microscopy image of human cornea see (Fratzl, 2008).

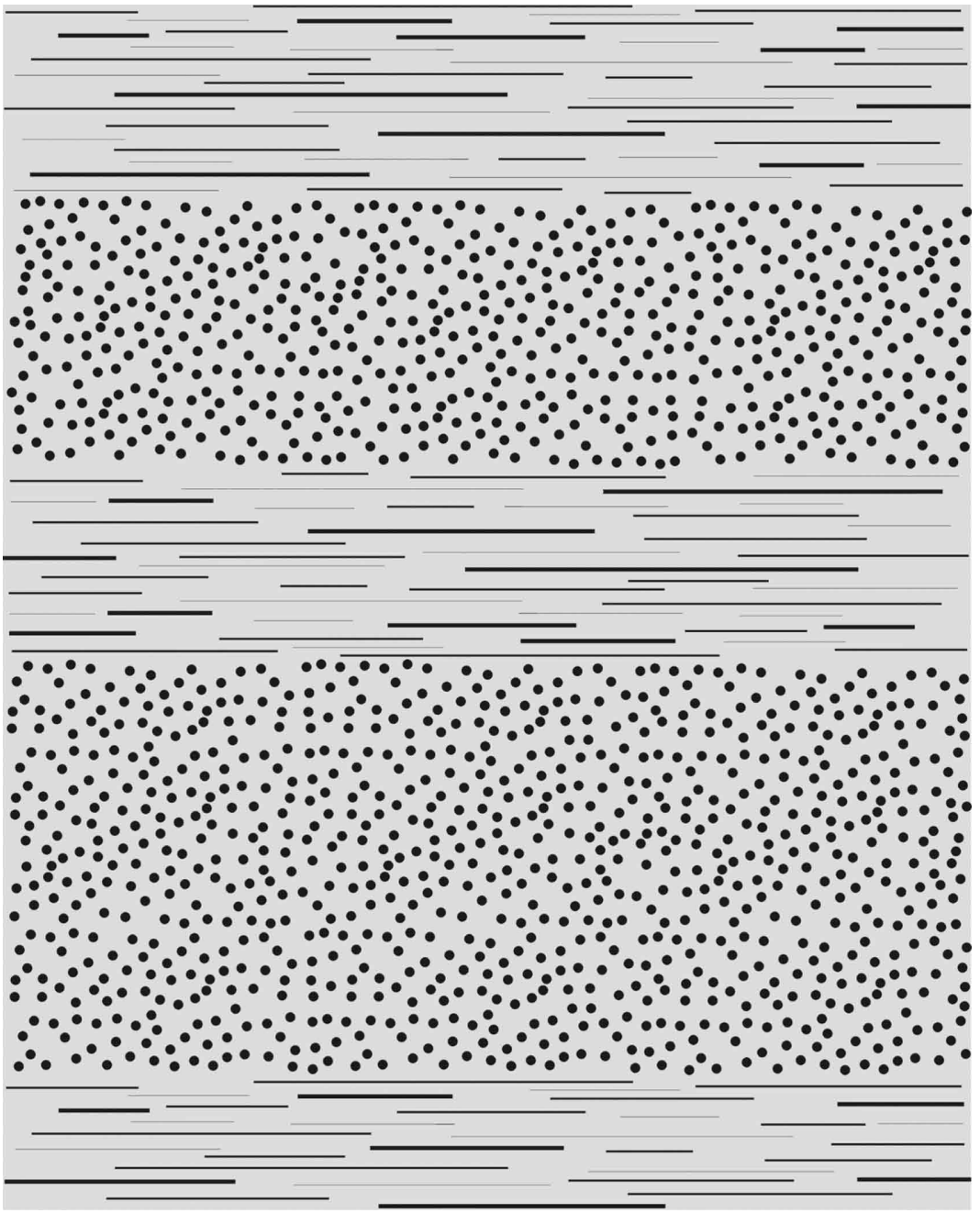

The *subendothelium of an artery* (a connective tissue between the endothelium and inner elastic membrane in the intima of arteries) consists of a multilayered fabric of collagen with larger variations in radial but also longitudinal orientations (Fratzl, 2008).

Figure 6. Circumferential (~) and radial (+) fibres at the optic nerve head. (Gogola, 2018): This work is licensed under a).

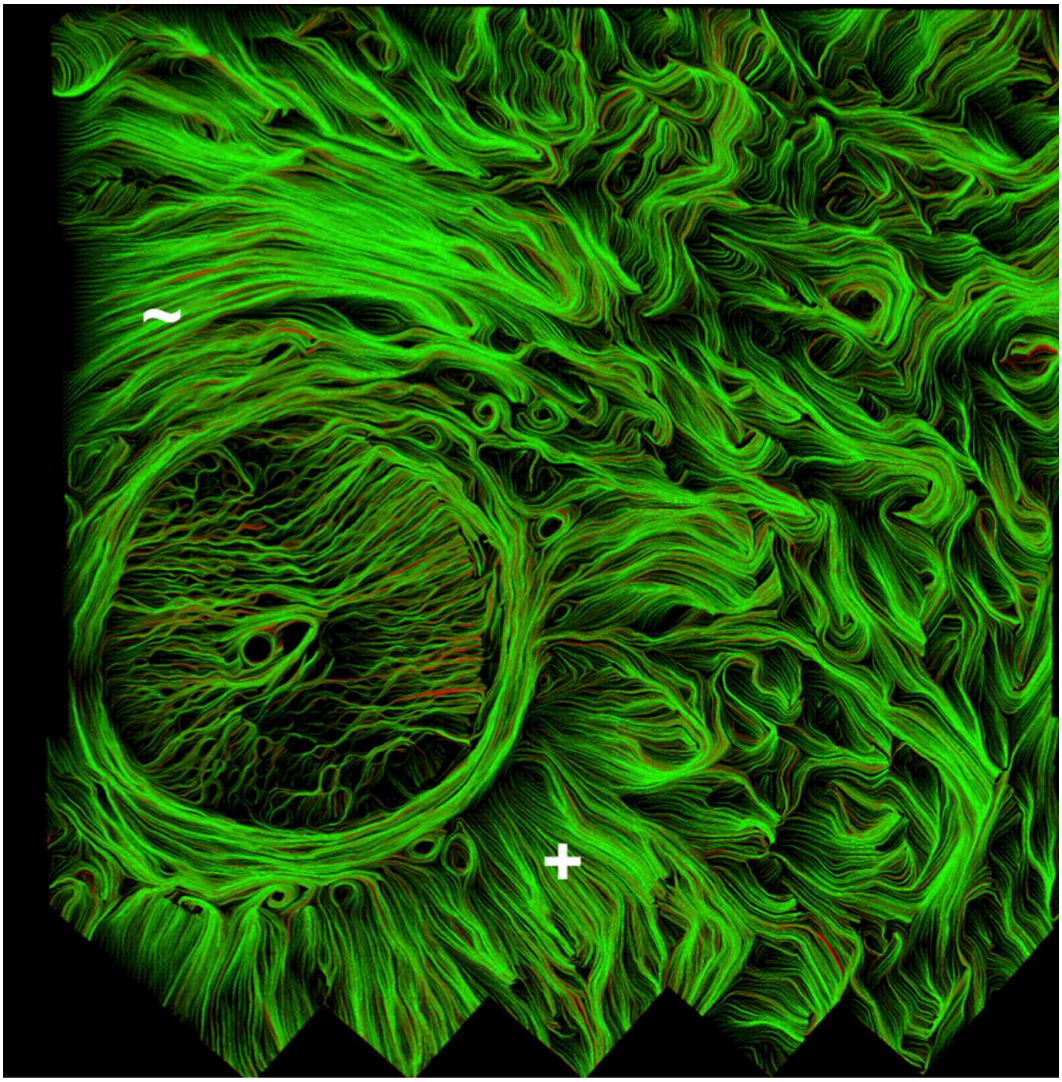

Collagen fibres in the sclera at the optic nerve head in the eye (Figure 6) arrange into two main orientations: circumferential fibres (~) around the optical nerve head and radial fibres (+) pointing out radially of the optic nerve head (Figure 6) (Gogola, 2018).

3. ARTIFICIALLY ALIGNED COLLAGEN TECHNIQUES

In recent decades, scientists and engineers have been very creative in developing a physical and chemical approach-based process spectrum, implementing various environments, for fabricating collagen constructs in 1D, 2D or 3D that mimic nature's collagen orientations and orientation distributions. For proving evidence on the success of these alignment strategies and for quantitative, comparable data on collagen alignment, various methods have been employed: polarization microscopy, polarization depended absorption spectroscopy, x-ray analysis, small angle x-ray scattering (SAXS), scanning electron microscopy (SEM), transmission electron microscopy (TEM),

atomic force microscopy (AFM), confocal reflectance microscopy (CRM), second harmonic generation (SGH) microscopy. Quantitative data from images were often accomplished by Fourier analysis (e.g. Fast Fourier Transform analysis (FFT)) by determining an order parameter.

Earliest attempts of fabricating scaffolds from collagen with an intrinsic orientation date back to 1964 by Benjamin et al. (1964) who implemented an electrical field.

3.1. 1-Dimensional Threads and Tubes

1D aligned collagen constructs in form of threads, nano-threads and tubes with an alignment orientation along the thread/tube direction have been fabricated by a variety of techniques, such as isoelectric focusing in an electrochemical cell and by extrusion.

3.1.1. Electrochemical

ELAC is the abbreviation for electrochemically aligned collagen. The group of Ozan Akkus has contributed substantially in this field. Cheng et al. (2008) have developed a method to fabricate short threats of collagen in an electrochemical cell. A fully dialysed tropocollagen (bovine hide) solution was placed between two electrodes about 1 mm apart on a glass slide. A voltage of 6 V was applied yielding a current through the collagen solution of 3.5 mA. The half-reactions resulting in the electrochemical cell generated a pH gradient between the electrodes: the anodic solution was acidic, the cathodic solution basic, which had a pronounced effect on the collagen. The collagen in the solution collected in a particular pH region via isoelectric focusing. The aggregated collagen molecules were oriented parallel to the electrodes (perpendicular to the electrical field lines) and closely packed uniformly across the entire thickness of the thread. Bundles several inches long with diameters between 50 - 400 μm could be fabricated by adjusting the electrode length and gap, as well as the current density. Treatment of the bundle in phosphate buffered saline (PBS) at 37°C for activation of fibrillogenesis and crosslinking in genipin solution was the last step of preparation and provided the final strength (Cheng, 2008). The mechanical properties of the ELAC fibers were systematically enhanced (Kishore, 2011) by adding inter-fiber cross linkers driving the bundle strength to values similar to a tendon's strength (Uquillas, 2012).

Nguyen et al. (2016) investigated the influence of elastin incorporation into ELAC threads, a composite for which a lower Young's modulus is achieved than that for tendons. They were interested in mimicking the much more flexible artery walls. By using a mixture of collagen/elastin (60/40 (w/w)) in an electrochemical cell they were able to decrease the Young's modulus to the required level. They could also show that smooth muscle cells were oriented along the fiber direction on pure ELAC collagen, however no orientation of the cells was found on the mixed ELAC material. Nevertheless, after 14 days of cell culturing cell orientation had taken place due to remodelling of the matrix and because the cells were sensing the underlying collagen orientation.

Younesi et al. (2014) improved the method for the fabrication of continuous ELAC threads exhibiting an excellent collagen orientation along the thread direction. The threads were fabricated with the help of a rotating electrode electrochemical alignment device (REEAD). The basic components of the REEAD are a syringe pump, a rotating electrode wheel and a collection spool. The syringe in the pump was loaded with the dialyzed collagen solution. The rotating electrode wheel had a circumferential groove housing two parallel electrode wires providing a quasi infinite electrode-length while rotating. The syringe pump applied the tropocollagen solution at the top of the wheel. The solution was trapped in the groove and between the electrodes while rotating with the wheel. During rotation in the electrical field, the collagen collected and aligned, resulting in the formation of the ELAC thread by the time the drum completed 1/3 of a turn (~60 s). The thread, after the 120 degree turn, was freed from the wheel and collected onto a spool. The diameter of threads could be controlled by the rotational speed of the wheel: higher speeds with less collagen led to thinner threads. Three diameters were fabricated: thin (0.10 ± 0.03 mm), medium (0.13 ± .04 mm) and thick (0.15 ± 0.05 mm). After thread formation the samples were incubated in PBS for 6 h at 37 °C

to induce fibril formation and then treated with 2-propanol solution for 12 h. Crosslinking of the ELAC threads was performed as the last step. These threads were stable enough to twist into yarns and weave into scaffolds.

In 2012 Kishore et al. (2012) demonstrated that artificial tendons, based on the ELAC method implanted into a rabbit's limb caused only low inflammatory response, were stable enough to serve as an implant and were degrading fast enough to allow the body's own tendons to take over. Therefore, the ELAC material seems to be biocompatible and biodegradable and opens the possibility of implementation in tendon tissue engineering.

3.1.2. Extrusion

Rat tail collagen in HCl was *coextruded* with a mixture of phosphate PBS and sodium phosphate in a 2 syringe system by Pins et al. (1997). The two liquids were combined at the end of the needle tips and forced through FEP (fluorinated ethylene propylene) tubing for extrusion into a flowing PB1 bath at 37°C. Long threads were allowed to form via self-assembly by immersion for 48 h in PBS. After rinsing in distilled water the threads were dried in air and stored. Before mounting of the threads in a custom made stretching device, the threads were re-immersed in PB and then stretched in 5% increments up to 50% of their original length and held at that extended length for 24 h in PB at 37°C. Some stretched threads were cross-linked by dehydration at 110°C in 5 days.

The various threads were tested with respect to their mechanical behaviour. Using polarization microscopy, the degree of fibril orientation within the threads was investigated. Stretched and un-stretched fibres showed a slight preferential alignment of the fibrils parallel to the thread direction. With increasing stress load the order of the alignment increased: for the non-cross-linked samples only very little, for the cross-linked samples substantially up to 30% stretching. Beyond the 30% stretch, the cross-linked samples lost some alignment and showed birefringence retardation values similar to original rat tail tendons. Encouraged by these results, Freeman and Silver (2005) studied the effect of the 30% stretching on the mineralization by calcium phosphate. They found that the higher order of the collagen fibrils in the threads led to a change in the calcium phosphate nucleation and growth, and that a higher organization with collagen-collagen interactions led to a better elastic energy storage.

In 2011 Lai et al. (2011) implemented an extrusion process with a special syringe, forming an extruded thin tube with a length in the order of 20 mm. For that rat tail collagen in acetic acid was used. The collagen solution was extruded with a flow rate of ~ 0.124 cm^3/s corresponding to a shear rate of the wall of ~220 s^{-1} in the thin annulus region of the syringe. As collagen was extruded through the annulus the inner rod became coated with a 0.5 mm thick layer of collagen. The rod with the collagen layer was immediately immersed in PBS at 37°C for 5 min inducing fibrillogenesis. Cross-linking was performed by either riboflavan initiated UV photo crosslinking, by dimethyl suberimidate, by a combination of both, by 1-ethyl-3-(3-dimethyl aminopropyl) carbodiimide hydrochloride (EDC) or by glutaraldehyde. Electron microscopy and FFT analysis revealed a preferential collagen fibril and fibril bundle orientation in the tubes along the tube axis with a ripple formation. The elastic moduli, the maximum extensibility and the burst pressure were studied and found to be partially depending on the cross-linking mechanism. The EDC cross-linking yielded an elastic modulus in the direction of the fiber orientation (along the axis of the tube) was in the order of 0.1-0.35 MPa, the maximum extensibility was ~ 0.14 and the burst pressure 12-28 kPa. Human fibroblast cells cultured on the collagen tubes showed a clear cell body orientation with the orientation of the collagen substrate indicating contact guidance induced by the anisotropy of the collagen.

3.2. 2-Dimensional Arrays (Sheets and Films)

2D collagen constructs with a single collagen orientation (e.g. samples with defined collagen orientation distributions in form of mats or sheets) have been fabricated by a variety of techniques: for example, by electrospinning and successive collection with a rotating wheel, by extrusion, by flow and evaporation induced orientation, stretching, AFM, Langmuir-Blodgett technology, electrostatic

interaction on mica, and by various processes inducing shear stress. There is a commercial product available from Advanced BioMatric, Inc., San Diego, US, called AlignCol® which consists of aligned-crimped type I collagen fibrils printed onto borosilicate glass with a thickness of ~ 1 μm, mimicking collagen fibril bundles represented in tendon, ligament, heart and other connective tissues.

3.2.1. Electrospinning

Electrospinning is a procedure that implements an electric field to manipulate the arrangement of polymers in a 1D thread and deposit the threads onto a 2D substrate, randomly or oriented. A polymer in solution or melted is ejected from a polymer reservoir with a nozzle, kept at a high electrical potential to create a charge imbalance, and captured on a grounded substrate. At a critical voltage, the surface tension at the nozzle is overcome by the charge imbalance leading to a jet of charged polymer. Due to the electrical field, the jet is directed toward the grounded substrate. In the case of a polymer solution, the jet also allows solvent evaporation and fiber formation. The electrospinning procedure creates a single continuous string. When choosing the right conditions in the polymer source and the electrospinning, the main chains are preferentially oriented along the thread direction. The substrate can be a grounded flat piece of material (2D) or a rotating spool that collects the thread like a yarn role (additional 1D methods).

In 2001, Matthews et al. (2002) employed *electrospinning* for fabrication of oriented 2D collagen nonwoven fabrics on a rotating substrate spool. They used collagen from calfskin and human placenta in acid soluble, lyophilized form. Collagen was dissolved at various concentrations in 1, 1, 1, 3, 3, 3 hexafluoro-2-propanol (HFP). Using a syringe pump, the collagen solution was delivered at varying rates (0 to 25 ml/h). An electric potential difference (15 -30 kV) was kept between the collagen source and the grounded rotating spool (~500 rpm) on which the collagen was collected. They were able to fabricate collagen mats with fibrils aligning linear, in parallel arrays. They found that the morphology of the collagen structure was depended on the chosen collagen source, but also on all fabrication process parameters.

In 2006, Zhong et al. (2006) reported on the fabrication of aligned nanofibrous collagen threads via electrospinning of calfskin collagen dissolved in HFP. The collagen suspension filled in a syringe with a G 27 needle was released at a speed of 1 ml/h via a syringe pump. A voltage of 15 kV was applied between the solution and the collecting spinning wheel (diameter: 0.2 m, grounded), which had a distance of 0.15 m from each other. The collagen fiber string approaching the collector wheel was attracted electrostatically to a glass coverslip on the wheel. The fibers where collected on the 2D-coverslip spinning with a speed of 15 m/s at the collecting rim. The fibers were aligned mainly along the rotation direction, clearly evident in SEM images. The samples on the cover slip were dried at room temperature for solvent removal. The collagen was cross-linked in glutaraldehyde vapor for 48 h, then immersed in aqueous glycine solution, rinsed with water, and finally dried in a vacuum. The spinning speed of the wheel is critical for the fiber alignment: too low a spinning speeds lead to poor orientation, too high a spinning speeds result in excessive forces and fibril rupture.

The density of these aligned collagen samples was systematically larger in comparison to unaligned electrospun samples prepared under identical conditions. The pores in-between individual fibers were much smaller in the aligned scaffold in comparison to non-aligned samples. Rabit conjunctiva fibroblasts showed a decrease in cell adhesion on aligned samples, but an increased proliferation in comparison to random collagen. The elongated proliferation pattern matched well with the cell morphology found in native tissue (Zhong, 2006).

Dong et al. (2009) used a similar rotating wheel electrospinning approach but substituted the corrosive and toxic HFP by a 1/1 (v/v) mixture of PBS and ethanol. They used bovine dermis tropocollagen. They found a dependency of the fiber diameter and its distribution on the salt concentration. With increasing salt concentration, the individual fiber diameter in the sheets decreased as well as the diameter distribution. Cross-linking was performed with 1-ethyl-3-(3 dimethylaminopropyl) carbodiimide hydrochloride and hydroxylsuccinimide in ethanol. Aligned

collagen was achieved by adjusting the rotation speed of the wheel onto which the collagen fibers were collected. Under these conditions, the collagen orientation aligned parallel to the spinning direction of the wheel, and parallel to the wheel surface. An order parameter of 0.97 was achieved (Dong, 2009).

3.2.2. Extrusion

A modified extrusion apparatus, equipped with two counter spinning cones between which collagen suspensions were extruded, was used to fabricate tubular collagen constructs by Hoogenkamp et al. (2015). These tubular constructs could deliver relatively large collagen sheets. They exploited bovine hide split collagen in an acetic/lactic acid mixture. The extruded film, still located on the inner cone, was immersed in NaCl solution for stabilization and storage (Hoogenkamp, 2015).

To define the zero angle (parallel to the extrusion direction, along the axis of the cones) for alignment studies with SHG microscopy and FFT analysis, and to test the influence of the cone spinning, a control sample was made with non-rotating inner and outer cones. It was found that the fibers in the control sample were oriented parallel to each other with an orientation parallel to the extrusion direction (0°), throughout the entire film (Hoogenkamp, 2015).

The samples prepared with rotating cones showed a distribution of alignment angles throughout the film. The alignment angle of the fibers located close to the outer cone ranged from 30° to 45°, changing to 0° within the central part and decreased to -20° to -35° at locations close to the inner cone. Mechanical properties depending on the extrusion conditions were studied (Hoogenkamp, 2015).

3.2.3. Magnetics

The diamagnetic anisotropy in proteins was described by Worcester (1978) in 1978. It results from the diamagnetic anisotropy of the planar peptide bonds of the proteins and has a negative value. This phenomenon drives the collagen - due to a torque appearing in a magnetic field - into an alignment perpendicular to the magnetic field. This behaviour was found by Murthy (1984) for collagen from rat tail tendon in acetic acid. The solution was concentrated by evaporation. Collagen films (0.15 - 0.25 mm thick) were produced via precipitation of collagen fibrils. Oriented collagen films (analyzed by polarization microscopy) were achieved by precipitating collagen fibrils within a magnetic field of 2 - 10 T with a fiber orientation perpendicular to the magnetic field (Murthy, 1984).

Torbet et al. (1984; 1986) found that collagen fibrils, prepared from lathyritic rat skin collagen in potassium phosphate buffer (pH 7.04) and heat-induced-reassembled in magnetic fields (1.9 and 5.6 T), were also oriented perpendicularly to the magnetic field and highly uniaxial. They assumed an enhanced diamagnetic anisotropy due to the large number of repeating units in the polymeric collagen, a process leading to a sufficient orientation energy to overcome kT, and the Brownian motion. In addition, they suspected further influence on the high orientation by the quartz cell surface holding the collagen sample.

3.2.4. Flow and/or Evaporation

Flow orientation of collagen during fibrillogenesis was used as early as 1972 by Elsdale et al. (1972). They mixed collagen from rat tail tendon to a solution of serum, Eagle's medium and NaOH at pH 7.6. The solution was cast onto a tilted substrate allowing the solution to drain during fibril formation. The resulting fibrils were oriented preferentially parallel to the draining direction. Human embryonic lung fibroblasts cultured on these aligned collagen samples showed a significant spindle form and aligned with the collagen orientation. A double layer sample was fabricated. The first layer of collagen was drained in one direction and fibroblasts cultured on top showing their characteristic shape and orientation. A second layer of collagen was prepared on top of the oriented cells (fibroblasts), and drained under an angle of 90° to the first draining direction. A second fibroblast culturing lead to a sample with crossed fibroblast orientations within the layers (Elsdale, 1972).

A simplistic approach of using moving magnetic beads (iron oxide) to introduce a flow environment was applied by Guo and Kaufman (2007). The beads were placed in a fibrogenic collagen

gel and driven by a very small magnetic field from a magnetic stir bar. This idea of flow-induced order originated from cell culturing approaches (Swartz's group (Ng, 2003; Ng, 2006)), implementing flow and leading to aligned cell scaffolds. 10 - 20 μm thin films of collagen (Vitrogen 100) in PBS with NaOH at pH 7.2 - 7.4 were placed between a microscope slide and a cover slip. Vitrogen 100 (Collagen, Palo Alto, CA) was a pepsin-solubilized collagen from bovine dermis which allowed to control the fibrillogenesis precisely within the necessary time window for alignment (Torbet, 1984). Magnetic beads with an average size in the order of 2.5 μm and various surface functionalizations were mixed into the collagen solution at concentrations between 0.01 and 0.1 mg/ml. A magnetic stir bar was placed on top of the cover slip (no motion). Fibrillogenesis was then initiated by heating the samples to 37°C in an incubator. With the help of CRM collagen fibril alignment was envisioned. Samples prepared without beads or without stir bar, and also fabricated with unmodified beads and the stir bar, showed randomly oriented fibrils. However, samples prepared with streptavidin-functionalized beats and the stir bar present depicted excellently high oriented fibrils. All other surface functionalities led to less orientation. The amount of beads and the strength of the magnetic stir bar played a role in the process. The orientation of the fibrils was found to be parallel to the magnetic stir bar and, therefore, parallel to the magnetic field lines of the bar. The magnetic field of the stir bar itself or the stir bar and the magnetic beads together are too small to align the collagen magnetically. The alignment was realized via the movement of the beads along the magnetic field lines through the collagen material, onto which the beads adhered via their surface functionalization, and was influenced by the binding capabilities of the beads to the growing fibrils. The mechanical moduli measured for these samples were similar to moduli of oriented collagen samples without beads. Embedded C6 Glioma cells in thick collagen samples either without or with iron oxide magnetic beads in the matrix, and a bead concentration of up to 0.2 mg/ml showed similar cell survival. The streptavidin-functionalized beads were nontoxic. The cells first aligned with the collagen, but then re-aligned the collagen, and decreased the order.

In 2009, Kirkwood and Fuller (2009) employed a flow and evaporation scheme with a robotic arm carrying a syringe. The syringe was fed with a collagen solution via a syringe pump. The robotic arm was programmed to follow particular paths on silica glass substrates while printing collagen solution from rat tail collagen in acetic acid. 18 - 27 gauge needles were used, bent in such a way that the liquid was dispensed parallel to the target surface. The movement speed was chosen between 20 - 100 mm/s and the flow rate of the collagen solution was adjusted between 0.05 - 0.5 ml/min.

The orientation of the printed collagen was characterized via AFM (tapping mode) and polarization microscopy. Two types of morphology were fabricated within a single printed stripe. The middle of the collagen stripe showed isotropic collagen whereas both sides of the stripe indicated clear cholesteric liquid crystalline fingerprints in form of parallel banding (polarization microscopy). However, the banding pattern found there was contrary to the banding occurring due to shear flow. In shear flow the banding of cholesteric liquids crystals appeared perpendicular to the flow direction, but here the collagen showed the banding parallel to the flow direction. The banding structure described a parallel collagen fibril orientation, which rotated helicoidally by moving perpendicular to the band structure, the so-called cholesteric axis. The distance under which the collagen fibrils undergo a 360° rotation is called the cholesteric pitch and is indicated by a change between dark/bright/dark positions in the polarization microscopy image (Kitzerow, 2001). Therefore, the collagen fibrils are always oriented (with respect to the substrate) in a plane perpendicular to the substrate and with this plane perpendicular to the flow direction. A twisted plywood structure perpendicular to the surface is fabricated with the cholesteric vector pointing perpendicular to the flow direction. A boundary condition is necessary to drive the system into the cholesteric phase, in the process of flow and solvent evaporation, and also to avoid the system to undergo a phase transition into a nematic phase. The contact line between the glass and the collagen solution offers this condition. The system can be tuned by experimental parameters including the collagen concentration. AFM images confirmed the high parallel alignment of the collagen fibrils in individual "layers" of the liquid crystal. Adult human

fibroblasts were cultured on top of a cholesteric collagen construct. The cells oriented themselves parallel to the banding structure and grew filopodia onto individual bands. The twisted plywood collagen structure has two physical features, which are possible reasons for contact guidance: there are different heights between bands and the collagen fibril orientation changes periodically.

An approach, where only evaporation was implemented to fabricate a cholesteric, twisted plywood structure, was discussed by Mosser et al. (2006). They constructed glass cuvettes that allowed the forming of a collagen concentration gradient by slowly delivering fresh collagen solution on one side and simultaneous evaporation on one or two sides of the cuvette. One cuvette was fed at the bottom via a small tube with collagen solution and allowed for evaporation at the open top. Collagen concentration enhancement was therefore, found at the top of the cuvette. The second cuvette was constructed as a wedge out of two glass slides with a distance changing from 1 mm to a few micrometers along the 30 mm side. The solution was delivered at the 1 mm opening. Evaporation occurred on both triangular sides of the wedge. Here the collagen was concentrated in the area of the small distance. Collagen from rat tail tendons in acetic acid was used and fibrillogenisis was induced by ammonia vapor leading to a collagen gel. In the fluid state, a transition of the collagen organisation was found with an increase in collagen concentration, like isotropic collagen, spherulites of local cholesteric organisation, aggregated spherulites forming a loose cholesteric organisation, larger aggregates with few defects, and finally a phase with a homogeneous unstructured birefringent response (Mosser, 2006). The fibrillary collagen gels were fixed with glutaraldehyde, uranyl acetate and osmium tetraoxide. Dehydration was performed in ethanol. Samples were then embedded in araldite and subjected to ultra microtome slicing. The slices were stained with toluidine blue (optical microscopy) or phosphotungstic acid (TEM). After fibrillogenisis the following structures were found with increasing collagen concentration: individual fibrils with twisted aggregated fibers, cholesteric spherulites, interconnected cholesteric domains, and large cholesteric domains with a cholesteric pitch and banded. The concentration of the collagen solution had an influence on the cholesteric pitch.

In this case of implementing an evaporation strategy for alignment, the surface of the cuvette also played an important role. The authors also found the necessary boundary condition of constrain; the cholesteric axis was always perpendicular to the interface with the glass or the air (Mosser, 2006).

3.2.5. Mechanical Stretching

Mechanical stretching was used by Falini et al. (2004) in collagen films made from equine Archilles' tendon in acetic acid. NaOH was added to the collagen solution to achieve pH 5, where precipitation of fibrils occurred. Films were formed from dried precipitate on centrifugation. For uniaxial stretching, films were cut into 6 x 25 mm pieces with a thickness of 0.1 mm. For stretching, the pieces were first immersed for 24 h in water, and then dried in air for 24 h while subjected to 4, 8 and 12% of strain. The strained dry collagen samples were compared to the natural tendon with respect to mechanical characteristics, denaturing temperature and structure. Strained samples were kept dry for all investigations because hydration caused swelling which led to a loss of the straining effects. In addition, in dry samples cross-linking of the fibrils seemed not to be necessary. The Young's modulus increased from ~1 GPa for the unstretched sample to 1.8 GPa for the 12% stretched sample, whereas the natural tendon showed ~5 GPa. The denature temperature increased by three degrees from the unstrained (98 °C) to the 4%-strained sample (111 °C). Further stretching led to another degree of temperature increase, while natural tendon showed 113 °C. SEM images indicated a fibular arrangement parallel to the strain direction. X-ray diffraction confirmed these data and exhibited a preferential orientation parallel to the strain direction of 0% for unstrained samples, 78% for the 4 and 8%-strained sample, and 83% for the 12% strained sample which was close to the 89% for the natural tendon. With this simple technique, the authors achieved collagen samples with similar attributes to the natural tendon material (Falini, 2004).

3.2.6. Langmuir-Blodgett-Technique

The first approach to deposit collagen by means of the Langmuir-Blodgett (LB) technology was carried out by Usha et al. (2004) in 2004 with the help of different structure modifiers like formaldehyde and basic chromium sulfate. They used rat-tail tendon in a solvent mixture of *n*-propanol/acetic acid. Following the spread of the solution on the air-water-interface of the LB-trough, the area-pressure-isotherm was studied. Native collagen and collagen treated with formaldehyde showed no phase transitions (gas-analog to liquid-analog to solid-analog) on the trough during compression whereas treatment with basic chromium sulfate led to a collagen phase transition behavior. LB-transfer took place on freshly cleaved mica. AFM investigations did not show alignment.

However, in 2010 Tenboll et al. (2010) showed that aligned collagen deposition on hydrophobic glass and quartz was feasible via the standard dipping procedure of the Langmuir-Blodgett technology with a film lift. They used collagen from rat-tail tendon in the *n*-propanol/acetic acid solvent mixture used by Usha et al. (2004). They first confirmed the non-denatured structure of tropocollagen in the used solvent mixture by circular dichroism spectroscopy. The LB films, fabricated with the film lift, consisted of a matrix of aligned tropocollagen containing embedded fibrillary aggregates. The orientation of the collagen was parallel to the dipping direction of the LB-deposition process. The LB-films were relatively thick; they did not depict monolayer format. The fibrillar aggregates formed during compression on the trough; fibrillogenesis was not triggered on purpose. In contrast, Langmuir-Schaeffer deposition of LB films on the air-water-interface did not lead to aligned collagen, as Sorkio et al. (2015) demonstrated. In addition, Tenboll et al. (2010) showed that the standard LB-deposited tropocollagen (without fibrilar aggregates) indicated a $\sin^2$ - behavior of a particular absorption feature in a series of absorption spectra (taken with a rotating polarization filter), clearly depicting the orientation of the tropocollagen along the dipping direction. AFM and SEM analysis confirmed the alignment of the tropocollagen matrix and the fibrillar aggregates. A cornea-like collagen structure (plywood) was fabricated by a double LB-deposition experiment with a 90° rotation of the substrate after the first deposition.

In 2013, the same group looked into the distribution of collagen orientation (tropocollagen and embedded fibrillar aggregates) and the orientation distribution on hydrophobic glass substrates using 'unusual' shapes (squares, triangles, circles, diamonds). Nahar et al. (2013) found that the alignment of the collagen is dictated by a convergent flow of the collagen layer on the trough towards and onto the substrate. In addition, the boundaries of the substrate contribute to the orientation distribution of the collagen on the substrate. They also found that these LB transferred structures are stable over extended periods of time at 37°C.

Ambrock et al. (2018) investigated the capacity of freshly prepared and aged collagen solutions to form oriented layers via LB-transfer on both hydrophobic and hydrophilic glass substrates. The pressure-area isotherms of the fresh and aged solutions showed some, but not substantial differences. Both materials formed aligned layers (tropocolagen matrix with embedded fibrillar aggregates) on hydrophilic and hydrophobic substrates. The replacement of n-propanol as a stabilizer by PBS in the subphase of the LB-trough led to nearly identical results. Small variations in film stability (possible ruptures during film transfer onto the substrate) occurred on very few of the different collagen/stabilizer/substrate formulations.

Ambrock et al. (2019) also investigated the aligned deposition of collagen onto substrates with patterns. Patterns were created by e.g. small hydrophobic areas in a hydrophobic substrate and vice versa. Small and large obstacles were formed by a solidifying gel placed onto the substrates, on all of these patterned samples, the LB-transfer produced homogeneously aligned collagen samples. Only in cases of a dense row of small obstacles or a very large obstacle in the middle of the sample, the convergent flow of the collagen onto the substrate was disrupted and led to an incomplete coating with flow alignment around the obstacles (quasi circumferential). The inner cohesion of the formed collagen LB-film on the trough is very high, even without purposely-triggered fibrillogenesis, so that relative large forces are necessary to disrupt the film. This is a valuable insight into the LB-

film behavior, as the method should allow for coating more sophisticated substrates, for example 3D-implants with irregular shapes or structures with holes.

In 2013, Pastorino et al. (2014) used LB-technology for film production using a layer-by-layer approach of alternating collagen and hyaluronic acid. They implemented collagen from calfskin in an n-propanol/acetic acid solution. The pressure-area isotherm for collagen was featureless as previously reported (Tenboll, 2010; Nahar, 2013; Ambrock, 2018). The collagen was transferred to a silicon substrate via Langmuir-Schaefer transfer. Using AFM they found aligned collagen patches in sizes of > (10 μm x 10 μm), the orientation direction was different for each individual sample. They claim this is due to operator-dependence of the Langmuir-Schaefer transfer. Sorkio et al.'s (2015) results showed orientation in aligned domains, but an overall statistical process. 3T3 mouse fibro-blast cells were cultured on the collagen coated and un-coated silicon substrates. The collagen coated substrates showed excellently adhering cells whereas on silicon only a few cells adhered. Depending on the precise collagen deposition protocol (with and without hyaluronic acid and amount of deposited layers), cells showed no, some or good alignment over areas > (200 μm x 200 μm).

3.2.7. Electrostatic Interaction on Mica

The strong Coulomb interactions between collagen and mica was used by Sun et al. (2008) in fabricating aligned collagen fibrils along a specific crystallographic axis of mica. They first mixed collagen (Vitrogen) in HCl solution. The collagen was then further dissolved in sodium-containing phosphate buffer before deposition on freshly cleaved mica. Following a 15 min incubation, the mica samples were rinsed with the buffer and then incubated again overnight in buffer solution. Analog samples were fabricated using a potassium-containing phosphate buffer. The AFM images of these samples showed collagen fibers all aligned parallel to each other, but indicating different individual length (in the μm regime) and fibril density. These fibrils were found on samples with the buffer present and in the dried state. Laue diffraction experiments show that the fibrils were aligning parallel to the direction on the reconstructed mica lattice. The samples fabricated with the sodium buffer showed significantly better-aligned fibrils than samples treated in the potassium buffer. The authors concluded that besides the electrostatic interaction between the freshly cleaved mica and the tropocollagen, sodium ions play a role in the alignment process of the fibrils.

3.2.8. AFM

Jiang et al. (2004a) achieved similar results as Sun et al. (2008) by pre-growing collagen samples on mica. They used dermal collagen from bovine in PBS and flushed it, creating a hydrodynamic flow, over freshly cleaved mica for 10 min before rinsing. Using AFM, they found aligned fibrils on mica, with an alignment direction parallel to the flow direction. The pH of the collagen solution was varied from pH 5.5 to pH 9.5. It was found that the oriented collagen fibrils started to form at pH 6.5. Above pH 8.5 the fibril density on the mica depends on the pH value. Above pH 10.5, and below pH 6.5 no fibrillar structures were observed. A closer look at some structures formed on the mica revealed fibrils with a width larger than 20 nm, and were therefore called ribbons (Jiang, 2004a).

After pre-growth of the oriented fibrillar structures on mica, Jiang et al. manipulated the orientation of the collagen fibrils by an AFM tip via scanning a defined area within the sample using a high load of 300 pN under buffer. The fibrils were than scanned with the AFM by a low load (100 pN). In the manipulated areas, the collagen fibril orientation was parallel to the scanning direction of the high load AFM tip. The manipulation of the collagen fibrils was possible in any direction relative to the starting orientation. Height measurements confirmed no changes in the fibrils besides the orientation, however sometimes a decrease in fibrillary density was observed. This AFM manipulation of collagen orientation was possible only with fresh collagen samples. After 4 - 5 h, manipulation was impossible, even with extreme loads of 2000 pN. The freshly manipulated samples and their orientation patterns were stable over at least 8 weeks.

By choosing the pH (2.5 - 10.5) and different salts ($MgCl_2$, NaCl, KCl) and concentrations thereof in the collagen solution, the fibril density, the self-assembly of the collagen fibrils, and their orientation could be controlled (Jiang, 2004b) directly on mica by flow induction. Potassium ions in the collagen solution led to a periodic pattern of ~ 66 nm repetition length in collagen ribbons. Jiang et al. (2004b) propose that a correct lateral assembling of collagen fibrils forms a D-period in the ribbon.

Later, Pool et al. (2005) created AFM oriented collagen with and without D-periodicity and showed that mouse dermal fibroblast cells grew in an oriented fashion only on the collagen with the D-periodicity. If, in addition, an RGD peptide with a single binding moiety was used during cell culturing, cell binding was, in general, not jeopardized, but a loss in orientation along the collagen fibrils occurred. Individual motile cells showed a preferential movement parallel to the collagen fibril alignment only in cases where a D-period was present in the aligned collagen structures.

3.2.9. Spin-Coating – Flow Induced Shear Forces

Lee et al. (2006) and Saeidi et al. (2009) performed collagen alignment studies based on flow induced shear forces in a microchannel on glass substrates. They prepared a monomeric solution of atelocollagen at pH 2, (collagen from Biomaterials, Fremont, CA) diluted in PBS. They found collagen fibril alignment mainly parallel to the flow direction depending on the shear rate. For modeling the collagen behavior in the microchannel, collagen molecules were treated as semi-flexible polymer chains. The authors distinguished between non-tethered chains flowing in the bulk solution, and tethered chains immobilized at the cuvette's surface under Poiseuille flow conditions. The simulations confirm the experimental results. D-banded fibrils were only found under no-flow conditions. Based on these results, Saidi et al. (2011) introduced the spin-coating technique, known for a long time, to produce anisotropic polymer orientation with a preferential alignment parallel to the substrate (Paul, 1996) and a radial distribution within the substrate plane, as a true 2D collagen film fabrication method. They fed the collagen solution with controlled flow rates (0.3 - 1 ml/min) centrally and in a continuous fashion onto the surface of the rotating disc placed on the rotation axis of the spin coater. The spin speed was adjusted between 750 and 3000 rpm, and the coverslip to be coated was mounted off-axis onto the rotating disc to achieve a collagen orientation in a semi-radial fan like way. This approach delivered locally aligned collagen fibrils under very distinct conditions of feed flow rate and spinning speed. Best orientation results were achieved at 1000 rpm. At the highest spin speed, no self-assembly of the collagen or any aggregation was found over substantial areas of the coverslips. The authors found that alignment of spin-coated collagen fibrils was highly dependent on both the hydrodynamic shear stress and the hydrodynamic confinement (thickness of rotating collagen solution). To mimic cornea, which exhibits an orthogonal pattern of parallel aligned collagen fibril layers with 90° rotations between successive layers (plywood), the coverslips were rotated 90° between individual layer formation. The authors discuss the advantages but also the problems arising using spin-coating: the stability of the spinning fluid film played a key role in the uniformity of the collagen deposition and the overall orientation distribution of the self-assembled collagen fibrils. Instability of the rotating fluid film could be due to an unstable rotating disc, and vibrations resulting in uneven deposited collagen amounts causing asymmetric shear rates. The deposition of stable thin films via spin-coating onto solid substrates is a highly complex phenomenon.

3.2.10. Shear Forces on Collagen in Liquid Crystalline Form

In a series of patents Paukshto et al. (2009; 2001; McMurtry, 2011) showed that acetic acid collagen solution with and without additives could be concentrated to form liquid crystal, either nematic or cholesteric. The liquid crystal was used for coating of solid substrate surfaces (glass, polymers, semiconductors, and biomaterials). The coating was conducted by applying a shear force to the liquid crystal using the slot die technology or a liquid film applicator assembly (McMurtry, 2011), which typically aligns the collagen in the direction of the coating. However, by fine-tuning the coating conditions (substrate, collagen concentration, gap between surface and flat phase of coating head, and coating speed) woven structures were also possible.

3.2.11. Inkjet Printing

Deitch et al. (2008) had implemented an inkjet printer for printing aligned collagen onto glass. To accomplish that task, rat-tail collagen (in acid) was used. A HP DeskJet 500 (C2106A, Hewlett-Packard) was operated in an incubator for humidity control. It was modified with new gear mount pillars possessing increased tolerances. A thoroughly cleaned ink cartridge was used to print a pattern of 8 parallel 20 μm wide horizontal lines. By staining with mouse monoclonal anti-collagen type 1 (an antibody that did not bind to denatured collagen), intact, non-denatured collagen was proven in the printed lines. Polarization microscopy confirmed fibril formation and collagen orientation along the line direction. Cell experiments with neonatal rat cardiomyocytes delivered elongated cells in rod-like shapes parallel to the arrays of myofibrils in the printed lines.

3.3. 3-Dimensional Gels

A few attempts were made to create 3D collagen samples with collagen fibril orientation. Due to the 3D nature not only parallel alignments within a sheet or a thread were achieved but also circumferential and radial orientation typically by magnetic forces or by shear. Walters and Stegemann (2014) give an overview on general 3D alignment approaches, including molding, electrospinning, and mechanically controlled flow. In 3D collagen samples, typically hydrogels of collagen were fabricated. A hydrogel is a material that absorbs large quantities of water but still acts as a solid. The collagen phase of the hydrogel is only a tiny portion of the total mass and volume, however, maintains the hydrogel structure in a water-based environment. In collagen hydrogels, fibrils encapsulate water and avoid dissolution and swelling. Thus, the fibrils need to be entangled or chemically bonded to each other. Fibrillogenesis is therefore necessary for forming a 3D-hydrogel. Besides the established routes described by Walters and Stegemann (2014) there are a couple of other approaches to fabricate 3D oriented collagen constructs.

3.3.1. Magnetic

Girton et al. (1999) have used a hollow cylinder construct to fabricate 3D bulk collagen samples with circumferential or parallel arrangement by combining interfacial alignment effects with magnetic alignment. The collagen in a collagen gel will be oriented in the magnetic field during fibrillogenesis, which is controlled by temperature, pH and solvent concentration. The authors applied Vitrogen 100. For the circumferential samples, they used an outer cylinder of polypropylene that contained a Teflon rod. The HEPES-buffered collagen solution was filled into the space between the inner and outer cylinder and positioned in the magnetic field with the long axis of the cylinder-rod construct parallel to the magnetic field. The collagen aligns perpendicular to the magnetic lines and parallel to the Teflon surfaces. Therefore, an alignment of the collagen fibrils circumferential around the Teflon rod is produced. Without the inner rod, which selects the alignment direction from the plane perpendicular to the magnetic field, radial orientation would be expected. For parallel alignment, Girton et al. (1999) used a simple Teflon tube filled entirely with the collagen HEPES-buffer solution. The tube was placed in the magnetic field with the tube's long axis perpendicular to the magnetic field. A parallel collagen fibril orientation along the tubes axis occurred. By increasing the magnetic field, the birefringence of the collagen samples increased (Dubey, 1999).

Encouraged by the achieved 3D oriented samples, Dubey et al. (1999) studied neurite elongation into the magnetically aligned collagen rods. The depth of neurite elongation from chick embryo neurons into these rods was significantly larger than in controls (without magnetic alignment) and increased with increasing magnetic field.

Guo and Kaufman's 2D approach (Guo, 2007) of moving magnetic beads with various surface functionalizations in a small magnetic field can easily be expanded into 3D. A 1 cm diameter cylinder with a height of 1 cm was filled with collagen (Vitrogen 100) solution containing PBS, DMEM (modified basal eagle medium), fetal bovine serum, antibiotics, NaOH and iron oxide beads. A stir

bar, slightly stronger than in the 2D case, was placed close to the filled cylinder. Fibrillogenesis is triggered by heating the samples to 37°C. The results were comparable to the 2D approach: streptavidin coated beads led to the best alignment, parallel to the magnetic field lines of the stir bar. Spread C6 Glioma cells aligned well with the collagen alignment.

In 2018, Betsch et al. (2018) described a collagen-agarose hydrogel with embedded iron nanoparticles. This hydrogel was used in a 3D printer with an incorporated magnetic field to produce macroscopic 3D scaffolds with unidirectional aligned collagen fibers. The orientation of the collagen was introduced by the moving magnetic beads in the hydrogel along the magnetic field lines. Therefore, collagen fibrils were aligned parallel to the magnetic field lines. The mixture's concentration had a large influence on the alignment due to a varying viscosity. Both optical (SHG) and mechanical experiments confirmed the alignment. The aim was to produce a cartilage similar tissue. Therefore, human chondrocytes were successfully cultured inside the artificial tissue. The chondrocytes produced a glycosaminoglycan- and proteoglycan-rich matrix, which expressed characteristic markers. Constructs fabricated with two layers, one layer with collagen alignment and the second layer with a random collagen distribution, showed increased marker expression.

3.3.2. Temperature Gradient-Guided Thermal-Induced Phase-Separation Technique

In 2015 Chen et al. (2015) used pig tendon collagen in acetic acid to fill a round mold which consisted of a cold (-20°C) outer cylinder wall made from metal and a warmer inner polymer-rod. Lid and cap were also made from polymer for thermal insulation. Letting the collagen solution freeze from outside to inside (30 min) resulted in a radial-oriented crystallization of the collagen. After storing the material at -80 °C for more than 4 h, the crystallized materials were removed from the mold and lyophilized. After cutting into 5 mm thick cylinders they were thermally cross-linked. Electron microscopy revealed an excellent radial collagen fibril arrangement (fibril orientation from the inside of the cylinder to the outside).

3.3.3. Pneumatic Membrane Generating Vibrations

Hsu et al. (2015) implemented a two chamber cuvette with a flexible PDMS membrane separating both channels. One channel was used for pressured and frequency controlled air flow continuously relaxing and bulging the PDMS membrane into the second, the collagen channel. Integrated into the cuvette system was an indium-tine oxide based heater to allow temperature control (37 °C). 200 µl of bovin skin collagen in acidic acid was used to fill the collagen chamber. The collagen was vibrated at air pressures between ~13 - 68 kPa, with frequencies from 2 - 20 Hz for up to 45 min at 37 °C. After vibrations stopped, the collagen was kept at 37 °C for 4 h. The fabricated collagen gels showed parallel aligned collagen fibrils. The order parameter was depending on all parameters that were systematically changed in the study, and on the concentration of the collagen solution. The best degree of order in a sample was received with 20 Hz vibrations at a pressure of ~13 kPa. Unfortunately, the authors do not mention in which direction the orientation appeared within the sample: parallel or perpendicular to the bulging direction of the membrane!

A7r5 cells, cultured by Hsu et al. (2015) on ordered and random collagen samples, showed a similar growth rate and morphology. Cells did not show any favored direction on the random oriented samples; however, cells on the oriented collagen followed the alignment. Expression of proteins was studied too. The expression of α-actin and smoothelin proteins was very different. α-actin did not show a different expression level on oriented and random samples; however, the expression of smoothelin from cells on aligned matrices was higher than from cells on randomly collagen.

3.3.4. Flow Orientation

Rat-tail collagen solution in acetic acid was used by Isobe et al. (2012) and pushed through a robot-controlled polymer needle which was mounted to eject parallel to the deposition surface into a PBS solution for fibrillogenesis. The needle moved with a speed of 550 mm/s, while the PBS solution flow

was in opposite direction. This procedure delivered strings of collagen roughly 1 mm in diameter with a fibril orientation parallel to the "extrusion" direction, parallel to the string's long axis. After fibrillogenesis, the fibers were rinsed with water and arranged as (a) 1 dimensional bundles of strings, (b) 2 dimensional sheets with strings positioned side by side on a substrate, and (c) 3 dimensional blocks by positioning the strings layer-by-layer on top of each other. Tubes were manufactured as well. The manufactured scaffolds were dried in air and removed from the substrate. The authors were able to transplant a multilayered collagen tube as a blood vessel graft for the carotid artery into a rabbit.

3.3.5. Centrifugation

Zhang et al. (2017) centrifuged collagen from Leiocassis longirostris' skin in acetic acid using different forces, different temperatures and different durations. The centrifuge tubes were stored vertically for 24 h in an incubator at various temperatures. After hydrogel formation the samples were treated with 1-ethyl-3-(3-dimethylaminopropyl) carbodiimide (EDC) in PBS for 24 h and then dried. The collagen was aligned uniaxial along the long axis of the centrifuge tubes. Both SEM investigation and X-ray clearly showed the anisotropy of the artificial scaffold. TEM investigations showed a clear D-banding. Fibroblasts were cultivated on the scaffold (oriented and not oriented by omitting the centrifugation step). Morphology, proliferation and migration were tested on oriented and random scaffolds. With phase-contrast microscopy the spindle-shaped morphology of the fibroblasts was detected, however, on both the aligned and random samples.

3.3.6. Rotation of an Acupuncture Needle

In 2008, Julias et al. (2008) have used a stainless steel acupuncture needle under rotation to form a circumferential collagen orientation around the needle in a collagen gel. They used lyophilized collagen (Elastin Products, Owensville, MO) to form gel films with thicknesses of 2 - 6 mm. For assuring fibril formation, the samples were kept at 37°C for 2h. Cross-linking was achieved with formalin. Some samples stained with FITC-labeled collagen were used for confocal microscopy. The collagen gels were penetrated with the needle to insertion depths of 1.5 to 4.5 mm, corresponding to a penetration depth to thickness ratios from 25 - 75%. The orientation experiment was conducted in an inverted polarization microscope under crossed polarizers by rotating the needle motor-controlled with a rotation speed of 0.3 rev/s for 2, 4 and 10 rotations. In order to keep the needle position stable and avoid its back-rotation after decoupling the needle from the motor, a PDMS sheet was installed on top of the collagen sample which was penetrated by the needle as well.

The kinetic polarization microscopy yielded an increase in birefringence, an increase in alignment, with increasing amount of revolutions until the collagen gel failed (ruptures, creating a hole besides the needle) and the birefringence decreases. The birefringence patterns show a circumferential alignment of the collagen around the needle and transitions into a radial alignment with collagen rupture. The rupture happened always in the changeover zone between circumferential and radial. The number of rotations necessary for gel rupture did not depend on the collagen concentration, but strongly on cross-linking. Cross-linked samples ruptured at smaller revolution numbers than non-cross-linked samples. Confocal microscopy revealed a collagen density enhancement around the needle and a clear circumferential alignment close to the needle with a changeover to radial orientation with increasing distance to the needle (also before rupture). The birefringence increase was larger in non-cross-linked samples and scaled with the collagen concentration: higher collagen concertation led to higher birefringence. Also thinner gels showed more rupture stability and higher birefringence in comparison to thicker gels. Both storage and loss modulus increased significantly with both collagen concentration and cross-linking.

4. BRIEF OVERVIEW ON APPLICATION

There are studies conducted on various kinds of artificially aligned collagen scaffolds, trying to mimic natural tissue of a variety of organs. As applications of aligned collagen is not the scope of this review only a few examples are mentioned.

Fotticchia et al. (2018) used electrospinning to fabricate aligned tendon-like collagen tissue with a limited inflammatory response in a cell culture. Johnson et al. (2019) implemented a magnetically induced orientation of electro spun collagen fibers in a hydrogel in order to manufacture a scaffold for neuron guidance. Yao et al. (2015) used a longitudinally oriented collagen conduit combined with a nerve growth factor for nerve regeneration in a dog model. Zhou et al. (2018) created artificial "bone" by utilizing electrospun collagen as a host and precipitated hydroxyapatite nano-rods within the aligned collagen. The hydroxyapatite nano-rods were oriented along the collagen alignment and enhanced the mechanical properties of the scaffold significantly. Ozasa et al. (2018) fabricated aligned collagen constructs on a surface by inkjet printing and cultured undifferentiated human induced pluripotent stem cells (hiPSCs) on it. Osteogenic differentiation was induced during culturing to obtain osteoblasts (hiPSC-OBs) oriented parallel to the aligned collagen. The collagen matrix secreted by the hiPSC-OB cells was parallely aligned with the cellular orientation. The following mineralization process of hydroxyapatite delivered crystals with an orientation parallel to the collagen matrix and the cells, respectively, mimicking bone. Using electrospinning, Sun et al. (2018) manufactured oriented, random and 90° crossed aligned collagen scaffolds. The three kinds of scaffolds were cut into circular patches, sterilized and finally applied to artificially-made circular skin wounds of the same size in rat models. Clearly wound healing happened quicker for the aligned and 90°-cross-aligned scaffolds. Torbet et al. (2007) used magnetic collagen alignment to create a 3D scaffold. By allowing acid-soluble collagen to gel in a magnetic field and by combining a series of gelation–rotation–gelation cycles, a scaffold of orthogonal lamellae composed of aligned collagen fibrils was formed. The scaffold has been claimed to be a significant step towards the creation of a corneal substitute.

5. CONCLUSION

Collagen is one of the most understood proteins and has triggered a huge interest in engineering and designing artificial scaffolds and tissues from animal collagen for biomedical applications. Due to self-assembly behaviour into fibrous scaffolds, it makes the construction and fabrication of fibrous tissues relatively easy. Therefore, a variety of different approaches for alignment in 1D, 2D and 3D have been developed delivering nearly all kinds of collagen architectures, orientations and orientation distributions, as naturally found in human organs. Even micellar structures in solution were reported (Zhang et al., 2017).

The use of living cells to orient and/or re-orient collagen fibrils, from random to oriented or vice versa is not subject of this review, but another large field in tissue engineering to approach natural collagen orientations and orientation distributions (Mandal,1987; Walters, 2014; Abraham, 2007; Torbet, 2007; Iordan, 2010).

Despite of the many different methods applied for fabricating 1D, 2D or 3D-oriented macroscopic collagen samples, one main physical mechanism is applied: shear stress. Only magnetic orientation perpendicular to the magnetic field lines, ELAC orientation and the electrostatics on mica are exceptions. Mainly parallel, uniaxial arrangements have been described. Nature mimicking, more sophisticated structures are demonstrated, but they are still rare; e.g. circumferential structures and radial patterns were presented in a few cases only. The parameter spectrum for fabricating the oriented scaffolds is enormous: the sources of the collagen raw materials vary by animals and their organs, the temperature ranges from below zero to 37°C; the collagen media itself varies in concentrations, solvent mixtures, additives and pH, and the fibrillogenesis and cross-linking are triggered by many stimuli.

It is not clear at this point which of all the reported strategies will lead to implantable devices and where the pros and cons lie in each method as only a few attempts were followed through to the implant stage. No discussions about up-scaling "the production of aligned collagen constructs" are to be found yet, and no cost analysis has been conducted.

Although many successful attempts using cell cultures, and in-vivo applications of aligned collagen samples in animal models are found, neither standardized sterilization methods nor standardized procedures for testing key physical, biological and medical properties with respect to tissue engineering and implant technology are reported in the literature. However, one should expect more successful implementation of aligned collagen in the future, particularly in animal models. Immune reaction analysis and long-term studies need to be conducted. In addition, regulation about collagen recourses needs to be established. Despite the promises and attractiveness of collagenous artificial aligned scaffolds, there is still a long way to go until oriented collagen scaffolds will be used regularly and in a variety of tissues for medical treatments in humans.

ACKNOWLEDGMENT

The authors like to acknowledge Spencer Cook for helping with the literature search and Brian Davis for carefully adjusting the English.

REFERENCES

Abraham, L. C., Dice, J. F., Lee, K., & Kaplan, D. L. (2007). Phagocytosis and remodeling of collagen matrices. *Experimental Cell Research*, *313*(5), 1045–1055. doi:10.1016/j.yexcr.2006.12.019 PMID:17276428

Ambrock, K., Grohe, B., & Mittler, S. (2018). Controlling the hydrophilicity and cohesion during deposition of highly oriented type I collagen films: An approach for biomedical applications. *Thin Solid Films*, *656*, 75–82. doi:10.1016/j.tsf.2018.04.043

Ambrock, K., Grohe, B., & Mittler, S. (2019). Surface-modified substrates for the Langmuir Blodgett deposition of patterned ultra-thin and highly oriented collagen coatings. *International Journal of Surface Science and Engineering*, *13*(1), 14–36. doi:10.1504/IJSURFSE.2019.097912

Amiel, D., & Kleiner, J. B. (1988). Biochemistry of Tendon and Ligaments. In Collagen, Volume III Biotechnology. Boca Raton, FL: CRC Press.

Annaidh, A. N., Bruyere, K., Destrade, M., Gilchrist, M. D., & Ottenio, M. (2012). Characterization of the anisotropic mechanical properties of excised human skin. *Journal of the Mechanical Behavior of Biomedical Materials*, *5*(1), 139–148. doi:10.1016/j.jmbbm.2011.08.016 PMID:22100088

Benjamin, H. B., Pawlowski, E., & Becker, A. B. (1964). Collagen as temporary dressing and blood vessel replacement. *Archives of Surgery (Chicago)*, *88*(5), 725–727. doi:10.1001/archsurg.1964.01310230001001 PMID:14120696

Betsch, M., Cristian, C., Lin, Y.-Y., Blaeser, A., Schöneberg, J., Vogt, M., Buhl, E. M., Fischer, H., & Duarte Campos, D. F. (2018). Incorporating 4D into bioprinting: Real-time magnetically directed collagen fiber alignment for generating complex multilayered tissues. *Advanced Healthcare Materials*, *7*(21), 1800894. doi:10.1002/adhm.201800894 PMID:30221829

Brown, I. A. (1972). Scanning electron microscopy of human dermal fibrous tissue. *Journal of Anatomy*, *113*(2), 159–168. PMID:4577527

Chattopadhyay, S., & Raines, R. T. (2014). Collagen-based biomaterials for wound healing. *Biopolymers*, *101*(8), 821–833. doi:10.1002/bip.22486 PMID:24633807

Chen, P., Tao, J., Zhu, S., Cai, Y., Mao, Q., Yu, D., Dai, J., & Ouyang, H. W. (2015). Radially oriented collagen scaffold with SDF-1 promotes osteochondral repair by facilitating cell homing. *Biomaterials*, *39*, 114–123. doi:10.1016/j.biomaterials.2014.10.049 PMID:25477178

Cheng, X., Gurkan, U. A., Dehen, C. J., Tate, M. P., Hillhouse, H. W., Simpson, G. J., & Akkus, O. (2008). An electrochemical fabrication process for the assembly of anisotropically oriented collagen bundles. *Biomaterials*, *29*(22), 3278–3288. doi:10.1016/j.biomaterials.2008.04.028 PMID:18472155

Currey, J. D. (2002). *Bones*. Prinecton University Press. doi:10.1515/9781400849505

Deitch, S., Kunke, C., Cui, X., Boland, T., & Dean, D. (2008). Collagen Matrix Alignment Using Inkjet Printer Technology. *Proceedings of the Materials Research Society*, *1094*, DD07–DD16. doi:10.1557/PROC-1094-DD07-16

Dong, B., Arnoult, O., Smith, M. E., & Wnek, G. E. (2009). Electrospinning of nanofiber scaffolds from benign solvents. *Macromolecular Rapid Communications*, *30*(7), 539–542. doi:10.1002/marc.200800634 PMID:21706638

Dubey, N., Letourneau, P. C., & Tranquillo, R. T. (1999). Guided neurite elongation and Schwann cell invasion into magnetically aligned collagen in simulated peripheral nerve regeneration. *Experimental Neurology*, *158*(2), 338–350. doi:10.1006/exnr.1999.7095 PMID:10415141

Elsdale, T., & Bard, J. (1972). Collagen substrata for studies on cell behaviour. *The Journal of Cell Biology*, *54*(3), 626–637. doi:10.1083/jcb.54.3.626 PMID:4339818

Falini, G., Fermani, S., Foresti, E., Parma, B., Runini, K., Sidoti, M. C., & Roveri, N. (2004). Films of self-assembled purely helical type I collagen molecules. *Journal of Materials Chemistry*, *14*(14), 2297–2302. doi:10.1039/b401393j

Feng, L. (2010). *Multi-scale characterization of swine femoral cortical bone and long bone defect repair by regeneration* (PhD dissertation). University of Illinois, Urbana-Champaign.

Fotticchia, A., Musson, D., Lenardi, C., Demirci, E., & Liu, Y. (2018). Anisotropic cytocompatible electrospun scaffold for tendon tissue engineering elicits limited inflammatory response in vitro. *Journal of Biomaterials Applications*, *33*(1), 127–139. doi:10.1177/0885328218779846 PMID:29987990

Fratzl, P. (Ed.). (2008). *Collagen: Structure and mechanics*. Springer. doi:10.1007/978-0-387-73906-9

Freeman, J. W., & Silver, S. H. (2005). The Effects of prestrain and collagen fibril Alignment on in vitro mineralization of self-assembled collagen fibers. *Connective Tissue Research*, *46*(2), 107–115. doi:10.1080/03008200590954140 PMID:16019421

Gelse, K., Pöschl, E., & Aigner, T. (2003). Collagens - structure, function, and biosynthesis. *Advanced Drug Delivery Reviews*, *55*(12), 1531–1546. doi:10.1016/j.addr.2003.08.002 PMID:14623400

Girton, T. S., Dubey, N., & Tranquillo, R. T. (1999). Magnetic-induced alignment of collagen fibrils in tissue equivalents. In Methods in molecular medicine. Vol 18: Tissue engineering methods and protocols. Totowa, NJ: Humana Press Inc.

Gogola, A., Jan, N.-J., Lathrop, K. L., & Sigal, I. A. (2018). Radial and circumferential collagen fibers are a feature of the peripapillary sclera of human, monkey, pig, cow, goat, and sheep. *Investigative Ophthalmology & Visual Science*, *59*(12), 4763–4774. doi:10.1167/iovs.18-25025 PMID:30304458

Guo, C., & Kaufman, L. J. (2007). Flow and magnetic field induced collagen alignment. *Biomaterials*, *28*(6), 1105–1114. doi:10.1016/j.biomaterials.2006.10.010 PMID:17112582

Hamed, E., Lee, Y., & Jasiuk, I. (2010). Multiscale modeling of elastic properties of cortical bone. *Acta Mechanica*, *213*(1-2), 131–154. doi:10.1007/s00707-010-0326-5

Harkness, R. D. (1961). Biological functions of collagen. *Biological Reviews of the Cambridge Philosophical Society*, *36*(4), 399–463. doi:10.1111/j.1469-185X.1961.tb01596.x PMID:13904721

Harvey, A. K., Thompson, M. S., Cochlin, L. E., Raju, P. A., Cui, Z., Cornell, H. R., Hulley, P. A., & Sir Brady, M. (2009). Functional imaging of tendon. *Annals of the BMVA*, *8*, 1–11.

Hoogenkamp, H. R., Bakker, G.-J., Wolf, L., Suurs, P., Dunnewind, B., Barbut, S., Friedl, P., van Kuppevelt, T. H., & Daamen, W. F. (2015). Directing collagen fibers using counter-rotating cone extrusion. *Acta Biomaterialia*, *12*, 113–121. doi:10.1016/j.actbio.2014.10.012 PMID:25462525

Hsu, H. T., Rau, L. R., Zeng, Y. N., Kang, Y. L., Tsai, S. W., & Wu, H. M. (2015). External vibration enhances macromolecular crowding for construction of aligned three-dimensional collagen fibril scaffolds. *Biofabrication*, *7*(2), 025004. doi:10.1088/1758-5090/7/2/025004 PMID:25886195

Hulmes, D. J. S. (2008). Collagen diversity, synthesis and assembly. In P. Fratzl (Ed.), *Collagen: structure and mechanics* (pp. 15–47). Springer. doi:10.1007/978-0-387-73906-9_2

Iordan, A., Duperray, A., Gerard, A., Grichine, A., & Verdier, C. (2010). Breakdown of cell-collagen networks through collagen remodeling. *Biorheology*, *47*(5-6), 277–295. doi:10.3233/BIR-2010-0575 PMID:21403382

Isobe, Y., Kosaka, T., Kuwahara, G., Mikami, H., Saku, T., & Kodama, S. (2012). Oriented collagen scaffolds for tissue engineering. *Materials (Basel)*, *5*(3), 501–511. doi:10.3390/ma5030501 PMID:28817059

Jiang, F., Hörber, H., Howard, J., & Müller, D. J. (2004). Assembly of collagen into microribbons: Effects of pH and electrolytes. *Journal of Structural Biology*, *148*(3), 268–278. doi:10.1016/j.jsb.2004.07.001 PMID:15522775

Jiang, F., Khairy, K., Poole, K., Howard, J., & Müller, D. (2004). Creating nanoscopic collagen matrices using atomic force microscopy. *Microscopy Research and Technique*, *64*(5-6), 435–440. doi:10.1002/jemt.20101 PMID:15549696

Johnson, C. D. L., Ganguly, D., Zuidema, J. M., Cardinal, T. J., Ziemba, A. M., Kearns, K. R., McCarthy, S. M., Thompson, D. M., Ramanath, G., Borca-Tasciuc, D. A., Dutz, D., & Gilbert, R. J. (2019). Injectable, magnetically orienting electrospun fiber conduits for neuron guidance. *ACS Applied Materials & Interfaces*, *11*(1), 356–372. doi:10.1021/acsami.8b18344 PMID:30516370

Julias, M., Edgar, L. T., Buettner, H. M., & Shreiber, D. I. (2008). An in vitro assay of collagen fiber alignment by acupuncture needle rotation. *Biomedical Engineering Online*, *7*(19), 19. doi:10.1186/1475-925X-7-19 PMID:18606012

Kadler, K. E., Holmes, D. F., Trotter, J. A., & Chapman, J. A. (1996). Collagen fibril formation. *The Biochemical Journal*, *316*(1), 1–11. doi:10.1042/bj3160001 PMID:8645190

Kannus, P. (2000). Structure of the tendon connective tissue. *Scandinavian Journal of Medicine & Science in Sports*, *10*(6), 312–320. doi:10.1034/j.1600-0838.2000.010006312.x PMID:11085557

Kirkwood, J. E., & Fuller, G. G. (2009). Liquid crystalline collagen: A self-assembled morphology for the orientation of mammalian cells. *Langmuir*, *25*(5), 3200–3206. doi:10.1021/la803736x PMID:19437784

Kishore, V., Paderi, J. E., Akkus, A., Smith, K. M., Balachandran, D., Beaudoin, S., Panitch, A., & Akkus, O. (2011). Incorporation of a decorin biomimetic enhances the mechanical properties of electrochemically aligned collagen threads. *Acta Biomaterialia*, *7*(6), 2428–2436. doi:10.1016/j.actbio.2011.02.035 PMID:21356334

Kishore, V., Uquillas, J. A., Dubikovsky, A., Alshehabat, M. A., Snyder, P. W., Breur, G. J., & Akkus, O. (2012). In vivo response to electrochemically aligned collagen bioscaffolds. *Journal of Biomedical Materials Research. Part B, Applied Biomaterials*, *100*(2), 400–408. doi:10.1002/jbm.b.31962 PMID:22179969

Kitzerow, H.-S., & Bahr, C. (Eds.). (2001). *Chirality in liquid crystals*. Springer. doi:10.1007/b97374

Komai, Y., & Ushiki, T. (1991). The three-dimensional organization of collagen fibrils in the human cornea and sclera. *Investigative Ophthalmology & Visual Science*, *32*(8), 2244–2258. PMID:2071337

Kruger, T. E., Miller, A. H., & Wang, J. (2013). Collagen Scaffolds in bone sialoprotein-mediated bone regeneration. *TheScientificWorldJournal*, *812718*, 1–6. doi:10.1155/2013/812718 PMID:23653530

Kühn, K. (1986). The collagen family-variations in the molecular and supermolecular structure. *Rheumatology*, *10*, 29–69.

Lai, E. S., Anderson, C. M., & Fuller, G. G. (2011). Designing a tubular matrix of oriented collagen fibrils for tissue engineering. *Acta Biomaterialia*, *7*(6), 2448–2456. doi:10.1016/j.actbio.2011.03.012 PMID:21414424

Lee, C. H., Singla, A., & Lee, Y. (2001). Biomedical applications of collagen. *International Journal of Pharmaceutics*, *221*(1-2), 1–22. doi:10.1016/S0378-5173(01)00691-3 PMID:11397563

Lee, P., Lin, R., Moon, J., & Lee, L. P. (2006). Microfluidic alignment of collagen fibers for in vitro cell culture. *Biomedical Microdevices*, *8*(1), 35–41. doi:10.1007/s10544-006-6380-z PMID:16491329

Mandal, A. B., Ramesh, D. V., & Dhar, S. C. (1987). Physico-chemical studies of micelle formation on sepia cartilage collagen solutions in acetate buffer and its interaction with ionic and nonionic micelles. *European Journal of Biochemistry*, *169*(3), 617–628. doi:10.1111/j.1432-1033.1987.tb13653.x PMID:3691510

Marlow, F., Khalil, A. S. G., & Stempniewicz, M. (2007). Circular mesostructures: Solids with novel symmetry properties. *Journal of Materials Chemistry*, *17*(21), 2168–2182. doi:10.1039/b700532f

Matthews, J. A., Wnek, G. E., Simpson, D. G., & Bowlin, G. L. (2002). Electrospinning of collagen nanofibers. *Biomacromolecules*, *3*(2), 232–238. doi:10.1021/bm015533u PMID:11888306

McMurtry, D. H., Paukshto, M. V., & Bobrov, Y. A. (2011). *Liquid film applicator assembly and rectilinear shearing system incorporating the same.* US Patent Publication, 8028647 B2.

Mosser, G., Anglo, A., Helary, C., Bouligand, Y., & Giraud-Guille, M.-M. (2006). Dense tissue-like collagen matrices formed in cell-free conditions. *Matrix Biology*, *25*(1), 3–13. doi:10.1016/j.matbio.2005.09.002 PMID:16253492

Murthy, N. S. (1984). Liquid crystallinity in collagen solutions and magnetic orientation of collagen fibrils. *Biopolymers*, *23*(7), 1261–1267. doi:10.1002/bip.360230710 PMID:6466766

Nahar, Q., Quach, D. M. L., Darvish, B., Goldberg, H. A., Grohe, B., & Mittler, S. (2013). Orientation distribution of highly oriented type I collagen deposited on flat samples with different geometries. *Langmuir*, *29*(22), 6680–6686. doi:10.1021/la401421h PMID:23654220

Ng, C. G., & Swartz, M. A. (2003). Fibroblast alignment under interstitial fluid flow using a novel 3-D tissue culture model. *American Journal of Physiology. Heart and Circulatory Physiology*, *284*(5), H1771–H1777. doi:10.1152/ajpheart.01008.2002 PMID:12531726

Ng, C. G., & Swartz, M. A. (2006). Mechanisms of interstitial flow-induced remodeling of fibroblast–collagen cultures. *Annals of Biomedical Engineering*, *34*(3), 446–454. doi:10.1007/s10439-005-9067-3 PMID:16482410

Nygen, T.-U., & Bashur, C. A. (2016). Impact of elastin incorporation into electrochemically aligned collagen on mechanical properties and smooth muscle cell phenotype. *Biomedical Materials (Bristol, England)*, *11*(2), 025008. doi:10.1088/1748-6041/11/2/025008 PMID:26987364

Olsen, B. R. (1963). Electron microscope studies on collagen, 1. Native collagen fibrils. *Zeitschrift für Zellforschung und Mikroskopische Anatomie*, *59*(2), 184–198. doi:10.1007/BF00320444 PMID:13940064

Ottani, V., Martini, D., Franchi, M., Ruggeri, A., & Raspanti, M. (2002). Hierarchical structures in fibrillar collagens. *Micron (Oxford, England)*, *33*(7-8), 587–596. doi:10.1016/S0968-4328(02)00033-1 PMID:12475555

Ozasa, R., Matsugaki, A., Isobe, Y., Saku, T., Yun, H. S., & Nakato, T. (2018). Construction of human induced pluripotent stem cell-derived oriented bone matrix microstructure by using in vitro engineered anisotropic culture model. *Journal of Biomedical Materials Research. Part A*, *106*(2), 360–369. doi:10.1002/jbm.a.36238 PMID:28921822

Pastorino, L., Dellacasa, E., Scaglione, S., Giulianelli, M., Sbrana, F., Vassalli, M., & Ruggiero, C. (2014). Oriented collagen nanocoatings for tissue engineering. *Colloids and Surfaces. B, Biointerfaces*, *114*, 372–378. doi:10.1016/j.colsurfb.2013.10.026 PMID:24246194

Paukshto, M. V., & McMurty, D. H. (2009). *Oriented collagen-based materials, films and methods of making same.* US Patent, 2009/0069893A1.

Paukshto, M. V., McMurty, D. H., Bobrov, Y. A., & Sabelman, E. E. (2013). *Oriented collagen-based materials, films and methods of making same.* US patent, 8,492,332,B2.

Paul, S., Halle, O., Einsiedel, H., Menges, B., Müllen, K., Knoll, W., & Mittler-Neher, S. (1996). An anthracene-containing PMMA derivative for photoresist and channel waveguide application. *Thin Solid Films*, *288*(1), 150–154. doi:10.1016/S0040-6090(96)08823-2

Pinnell, S. R., & Martin, G. R. (1968). The cross-linking of collagen and elastin: Enzymatic conversion of lysine in peptide linkage to α-aminoadipic-δ-semialdehyde(allysine) by an extract from bone. *Proceedings of the National Academy of Sciences of the United States of America*, *61*(2), 708–716. doi:10.1073/pnas.61.2.708 PMID:5246001

Pins, G. D., Huang, E. K., Christiansen, D. L., & Silver, F. H. (1997). Effects of static axial strain on the tensile properties and failure mechanisms of self-assembled collagen fibers. *Journal of Applied Polymer Science*, *63*(11), 1429–1440. doi:10.1002/(SICI)1097-4628(19970314)63:11<1429::AID-APP5>3.0.CO;2-O

Polack, F. M. (1961). Morphology of the cornea. *American Journal of Ophthalmology*, *51*(5), 179–184. doi:10.1016/0002-9394(61)91794-9 PMID:13736666

Poole, K., Khairy, K., Friedrichs, J., Franz, C., Cisneros, D. A., Howard, J., & Müller, D. (2005). Molecular-scale topographic cues induce the orientation and directional movement of fibroblasts on two-dimensional collagen surfaces. *Journal of Molecular Biology*, *349*(2), 380–386. doi:10.1016/j.jmb.2005.03.064 PMID:15890202

Ramachandran, G. N., & Reddi, A. H. (Eds.). (1976). *Biochemistry of collagen*. Plenum Press. doi:10.1007/978-1-4757-4602-0

Ramshaw, J. A., Shah, N. K., & Brodsky, B. (1998). Gly-X-Y tripeptide frequencies in collagen: A context for host-guest triple-helical peptides. *Journal of Structural Biology*, *122*(1-2), 86–91. doi:10.1006/jsbi.1998.3977 PMID:9724608

Saeidi, N., Sander, E. A., & Ruberti, J. W. (2009). Dynamic shear-influenced collagen self-assembly. *Biomaterials*, *30*(34), 6581–6592. doi:10.1016/j.biomaterials.2009.07.070 PMID:19765820

Saeidi, N., Sander, E. A., Zareian, R., & Ruberti, J. W. (2011). Production of highly-aligned collagen lamellae by combining shear force and thin-film confinement. *Acta Biomaterialia*, *7*(6), 2437–2447. doi:10.1016/j.actbio.2011.02.038 PMID:21362500

Sherman, V. R., Yang, W., & Meyers, M. A. (2015). The materials science of collagen. *Journal of the Mechanical Behavior of Biomedical Materials*, *52*, 22–50. doi:10.1016/j.jmbbm.2015.05.023 PMID:26144973

Shoulders, M. D., & Raines, R. T. (2009). Collagen structure and stability. *Annual Review of Biochemistry*, *78*(1), 929–958. doi:10.1146/annurev.biochem.77.032207.120833 PMID:19344236

Simon, S. R. (1994). *Orthopedic Basic Science*. American Academy of Orthopedic Surgeons.

Smith, J. W. (1968). Molecular pattern in native collagen. *Nature*, *219*(5150), 157–158. doi:10.1038/219157a0 PMID:4173353

Sorkio, A. E., Vuorimaa-Laukkanen, E. R., Hakola, H. M., Liang, H. M., Ujula, T. A., Valle-Delgado, J. J., Osterberg, M., Yliperttula, M. L., & Skottman, H. (2015). Biomimetic collagen I and IV double layer Langmuir-Schaefer films as microenvironment for human pluripotent stem cell derived retinal pigment epithelial cells. *Biomaterials*, *51*, 257–269. doi:10.1016/j.biomaterials.2015.02.005 PMID:25771016

Sun, L., Gao, W., Fu, X., Shi, M., Xie, W., Zhang, W., Zhao, F., & Chen, X. (2018). Enhanced wound healing in diabetic rats by nanofibrous scaffolds mimicking the basketweave pattern of collagen fibrils in native skin. *Biomaterials Science*, *6*(2), 340–349. doi:10.1039/C7BM00545H PMID:29265119

Sun, M., Stetco, A., & Merschrod, E. F. (2008). Surface-templated formation of protein microfibril arrays. *Langmuir*, *24*(10), 5418–5421. doi:10.1021/la703292h PMID:18407679

Tenboll, A., Darvish, B., Hou, W., Duwez, A.-S., Dixon, S. J., Goldberg, H. A., Grohe, B., & Mittler, S. (2010). Controlled deposition of highly oriented type I collagen mimicking in vivo collagen structures. *Langmuir*, *26*(14), 12165–12172. doi:10.1021/la1018136 PMID:20560559

Torbet, J. (1986). Fibrin assembly in human plasma and fibrinogen/albumin mixtures. *Biochemistry*, *25*(18), 5309–5314. doi:10.1021/bi00366a048 PMID:3768349

Torbet, J., Malbouyres, M., Builles, N., Justis, V., Roulet, M., Damour, O., Oldberg, Å., Ruggiero, F., & Hulmes, D. J. S. (2007). Orthogonal scaffold of magnetically aligned collagen lamellae for corneal stroma reconstruction. *Biomaterials*, *28*(29), 4268–4276. doi:10.1016/j.biomaterials.2007.05.024 PMID:17618680

Torbet, J., & Ronziere, M.-C. (1984). Magnetic alignment of collagen during self-assembly. *The Biochemical Journal*, *219*(3), 1057–1059. doi:10.1042/bj2191057 PMID:6743242

Uquillas, J. A., Kishore, V., & Akkus, O. (2012). Genipin crosslinking elevates the strength of electrochemically aligned collagen to the level of tendons. *Journal of the Mechanical Behaviour of Miomedical Materials*, *15*, 176–189. PMID:23032437

Usha, R., Dhathathreyan, A., Mandal, A. B., & Ramasami, T. (2004). Behavior of collagen films in presence of structure modifiers at solid–liquid interface. *Journal of Polymer Science. Part B, Polymer Physics*, *42*(21), 3859–3865. doi:10.1002/polb.20191

Vuorio, E., & Crombrugghe, B. (1990). The family of collagen genes. *Annual Review of Biochemistry*, *59*(1), 837–872. doi:10.1146/annurev.bi.59.070190.004201 PMID:2197991

Walters, B. D., & Stegemann, J. P. (2014). Strategies for directing the structure and function of 3D collagen biomaterials across length scales. *Acta Biomaterialia*, *10*(4), 1488–1501. doi:10.1016/j.actbio.2013.08.038 PMID:24012608

Weiner, S., Traub, W., & Wagner, H. D. (1999). Lamellar bone: Structure-function relations. *Journal of Structural Biology*, *126*(3), 241–255. doi:10.1006/jsbi.1999.4107 PMID:10475685

Weiner, S., & Wagner, H. D. (1998). The material bone: Structure-mechanical function relations. *Annual Review of Materials Science*, *28*(1), 271–298. doi:10.1146/annurev.matsci.28.1.271

Weintraub, W. (2003). *Tendon and ligament healing, A new approach to sports and overuse injury*. Paradigm Publications.

Wenger, M. P. E., Bozec, L., Horton, M. A., & Mesquida, P. (2007). Mechanical properties of collagen fibrils. *Biophysical Journal*, *93*(4), 1255–1263. doi:10.1529/biophysj.106.103192 PMID:17526569

Worcester, D. L. (1978). Structural origins of diamagnetic anisotropy in proteins. *Proceedings of the National Academy of Sciences of the United States of America*, *75*(11), 5475–5477. doi:10.1073/pnas.75.11.5475 PMID:281695

Yao, Y., Cui, Y., Zhao, Y., Xiao, Z., Li, X., Han, S., Chen, B., Fang, Y., Wang, P., Pan, J., & Dai, J. (2015). Effect of longitudinally oriented collagen conduit combined with nerve growth factor on nerve regeneration after dog sciatic nerve injury. *Journal of Biomedical Materials Research. Part B, Applied Biomaterials*, *106*(6), 2131–2139. doi:10.1002/jbm.b.34020 PMID:29024435

Younesi, M., Islam, A., Kishore, V., Anderson, J. M., & Akkus, O. (2014). Tenogenic induction of human MSCs by anisotropically aligned collagen biotextiles. *Advanced Functional Materials*, *24*(36), 5762–5770. doi:10.1002/adfm.201400828 PMID:25750610

Zhang, J., Sun, Y., Zhao, Y., Wei, B., Xu, C., He, L., Oliveira, C. L. P., & Wang, H. (2017). Centrifugation-induced fibrous orientation in fish-sourced collagen matrices. *Soft Matter*, *13*(48), 9220–9228. doi:10.1039/C7SM01871A PMID:29199311

Zhong, S., Teo, W. E., Zhu, X., Beuerman, R. W., Ramakrishna, S., & Yung, L. Y. L. (2006). An aligned nanofibrous collagen scaffold by electrospinning and its effect on in vitro fibroblast culture. *Journal of Biomedical Materials Research. Part A*, *79*(3), 456–463. doi:10.1002/jbm.a.30870 PMID:16752400

Zhou, Y.-Y., Li, S., Wang, D.-L., Han, X., & Lai, X. (2018). Fabrication of collagen/HAP electrospun scaffolds with perfect HAP nanorods along nanofiber orientation. *Science of Advanced Materials*, *10*(7), 930–936. doi:10.1166/sam.2018.3278

Karina Ambrock is a master student at UWO, London, Ontario, Canada and a PhD student at University of Muenster, Germany.

Bernd Grohe is a researcher in Germany and Canada since the 1990s.

Silvia Mittler is a Full Professor at Physics and Astronomy at the University of Western Ontario since 2003.